2018

Effect Of Weak Adhesion Interface On Mechanical And Dielectric Properties Of Composite Materials

Prashant Katiyar
University of South Carolina

EFFECT OF WEAK ADHESION INTERFACE ON MECHANICAL AND DIELECTRIC PROPERTIES OF COMPOSITE MATERIALS

by

Prashant Katiyar

Bachelor of Science
Barkatullah University, 2009

Submitted in Partial Fulfillment of the Requirements

For the Degree of Master of Science in

Mechanical Engineering

College of Engineering and Computing

University of South Carolina

2018

Accepted by:

Prasun Majumdar, Director of Thesis

Xinyu Huang, Second Reader

Cheryl L. Addy, Vice Provost and Dean of the Graduate School

ACKNOWLEDGEMENTS

First of all, I would like to express my earnest gratitude to Dr. Prasun Majumdar for his continued guidance throughout my research endeavors. I'm forever inspired by his drive to learn something new every day and his vast knowledge in the field of advanced materials. I'd like to thank Dr. Xinyu Huang for being a part of my thesis defense committee.

Next, this research would not have been possible without the unending encouragement and assistance from my colleagues – Shriram Bobbili, Alice Arnold and Cameron Wilkes.

Lastly, I would like to thank my family, especially my sister for motivating me and supporting me throughout my studies here in USC.

ABSTRACT

Interfaces are often the most critical part of the heterogeneous materials and their structures. Such interfaces appear a multiple length scales and significantly affect bulk properties in different material systems. Fiber reinforced composite materials are one such example of heterogeneous materials with interfaces at constituent scale (fiber-matrix interface and interphase) to laminate scale (secondary adhesive joints). Manufacturing induced defects and subsequent in-service damage at these interfaces can severely affect the durability of fiber reinforced laminated composite materials and their joints. In addition to lamination process, defects can also form during secondary joining process (e.g., adhesive bonding and repair) which can be very detrimental to the performance of the composite structure as it can become the "weak link". Adhesive bonding has wide applications in different disciplines including bio-medical, energy, automotive, civil and aerospace structural composites. With growing popularity of adhesive bonding, manufacturing defects at the interfaces of joints have attracted increased attention of many researchers in the recent years. Although significant progress has been made in detecting specific types of defects such as voids and large debonding using different NDE methods, there is a lack of understanding of so called "zero volume" defects which forms a weak interface. The purpose of this study is to examine the role of defects at the adhesive-to-laminate interface on multi-physical properties, and specifically understand how a weak interface may affect mechanical durability.

In this study, a multi-faceted approach has been taken to understand fundamental scientific challenge of surface properties and its implications on bonded interface. Controlled experiments have been designed to create weak interface by different surface modification technique and validated with indirect measurement of work of adhesion. Using broadband dielectric spectroscopy (BbDS) technique, the effect of surface modification on dielectric properties are quantified. This modification is then translated in formation of a truly “weak interface” with “zero volume” unlike a traditional disbond or delamination type scenario. The laminated composite joint is then studied for both mechanical and dielectric property changes due to the formation of weak interface. Carbon fiber reinforced laminate and epoxy adhesive were taken as test bench material systems although the fundamental focus is not on the material itself but the interface.

Interface strength of bonded joint was determined experimentally and quantitatively linked to dielectric properties. Several analytical models were developed to understand the effect of weak interface on dielectric properties and results demonstrate that the model captures observed experimental trend of property changes. Moreover, failure of bonded structure under tension loading was also predicted with analytical tools available in the literature and it was observed that only shear dominated brittle fracture represents the weak interface adequately. This is an interesting shift as a strong joint will show ductility in terms of both shear and peel stresses due to adherend bending effect. Details of experimental results and analyses of weak interface have been included in this thesis.

TABLE OF CONTENTS

LIST OF FIGURES

LIST OF TABLES

CHAPTER 1

INTRODUCTION AND LITERATURE REVIEW

1.1 Introduction

Composite materials are widely used in various fields as the ability to select required material composition depending on the application and creating a tailor-made structure for specific utility is extremely useful. One of the primary advantages of composite materials is the ability to obtain high strength while maintaining a relatively low density. One such example is the ability of a basic for of carbon fiber being able to match the strength of high rage aluminum in all directions at less than half their density. The other primary advantage is the ability to customize the layup of the materials to better suit requirement; for example, a unidirectional carbon fiber composite has more than double the strength and stiffness of steel. Finally, composite materials can be easily modified to provide better resistance to environmental degradation [6].

Fiber reinforced polymer composite materials are primarily composed of the fibers and the matrix with the option of adding additional secondary materials to further improve the required properties. The fibers are the primary source of strength and stiffness. They can also be coated with other substances to increase bonding with the surrounding matrix. The matrix is the primary minding agent that holds the fibers together. It protects the fibers from abrasion, provides inter laminar shear strength and helps transfer loads in between the fibers. Finally, additives and fillers can be used to incorporate additional specific properties such as fire resistance, corrosion resistance, etc. [7]. The combination

of unidirectional or woven fiber, matrix and secondary substances to create a flat or sometimes curved panel is called a lamina. A combination of these lamina arranged in their specific orientations to achieve required properties is called a laminate. The properties of the laminate depend on both the lamina properties and the stacking sequence of the fibers.

With increasing application of carbon fibers reinforced composites in advanced industries, i.e. aerospace, automobiles and civil infrastructure, the priority for structural engineers is to come up with novel joining technology to assist fabrication of large structures. Conventional materials like steel or aluminum are mechanically joined by fasteners, welding, etc., but these joining methods are not favorable for CFRP parts as machining (drilling or cutting) can cause damage and affect performance. Adhesive joining of composite structures is gaining popularity because of various advantages it offers over traditional mechanical methods, like lower structure weight, reduced stress concentration, improved damage tolerance, etc. Adhesives are organic polymeric materials which undergo a polymerization reaction during curing to become a thermoset plastic.

1.2 Literature review on adhesive bonding in composites

Composites have experienced a steady growth over the last several decades now, not only in small application but also large-scale structures like turbines, rockets, and submarines, due to advantages like light weight, high stiffness, etc. Two types of assembly methods are commonly used for integration of composite parts: mechanically fastening and adhesively joining of composites. Mechanical fasteners' advantages include easy straightforward design, on-site assembly and repair, and easy inspection [25]; however, fasteners are prone to fatigue and corrosion, can initiate complex damages inside the

laminate, and are limited to thicker laminate use only. Also, they are not as effective in composites as in metallic structures [25, 26]. Adhesive bonding offers various advantages [9] over mechanical fastenings methods, notably:

- Uniform stress distribution over joint length
- Improved fatigues and impact performance
- Vibration damping
- Adhesive bond acts as a sealant and as a corrosion resistant
- Unlike welding, no adherend distortion during bond formation
- Different kinds of material can be joined
- May allow reduction of manufacturing cost of structure

Adhesive bonding was primarily used by aerospace industries in place of traditional joining methods such as riveting. In adhesive joints, adherends are composite parts joined by the adhesive. The mechanical properties of the adherend and adhesive govern the strength of the adhesive bond. The bond durability of adhesive joints depends on various parameters like surface preparation of adherend, type of materials to be joined, adhesive preparation, bond line thickness, clamping pressure, cure time and temperature [1-4]. Adherend surface preparation for bonding is one of the most critical factors deciding the quality of the joint. During manufacturing of composite joints, defects at the interface due to poor surface preparation can be detrimental to the structure [5]. Prior surface treatment of adherend surfaces can provide high surface energy and significantly improve the bond strength [8]. There are various pre-treatment processes like grit blasting, corona discharge, acid etching, laser treatment, etc., to ensure the surface is free from contaminants like oil, grease, mold release agents, etc., that help prevent premature joint failure. The goal of

surface preparation for composites is to raise the surface energy of adherend to enhance bonding without damaging the fibers in the laminate. Most surface pre-treatments provide optimal surface preparation for bonding, but they have limited shelf life [8]; therefore, any contaminant removal should be done prior to bonding. Previous researchers [10] suggested that carbon fiber composites require only a simple pretreatment of surface abrasion and solvent wiping prior to bonding.

Adhesively bonded joints can be designed depending upon loads and type of application. Common types of joints include single-lap, double-lap, stepped, scarf, tapered scarf, T-shaped, etc. A detailed study of composite joints design under different loadings is discussed by Chamis and Murthy [11]. Single-lap joints are most commonly used due to their simplicity and are also used in this study. Due to its simple design and fabrication, single lap is the most common of all joints [12].

Durability of adhesively bonded composite structure under demanding application is extremely important and depend on the quality of bond manufactured. Defects can be produced in adhesive joints during the manufacturing process and can potentially affect their functional life. The primary modes of failure (figure 1.1) in adhesive bonds [13] are:

1. Cohesive failure: Failure occurring primarily in adhesive layer. This is considered optimum type of failure if adhesive bonded joint fails at predicted load.
2. Adherend failure: Interlaminar failure in composite structures.
3. Adhesive failure: Failure between adhesive and adherend interface.

Failure at the adhesive layer or cohesive failure is considered design related failure and can be overcome by selecting appropriate adhesive material with properties according to the type of application. The strength at the interface between adhesive and adherend in

an adhesive bond is most critical to overall joint strength, and it is considered the limiting factor in the bond performance. The interfacial strength can be affected by

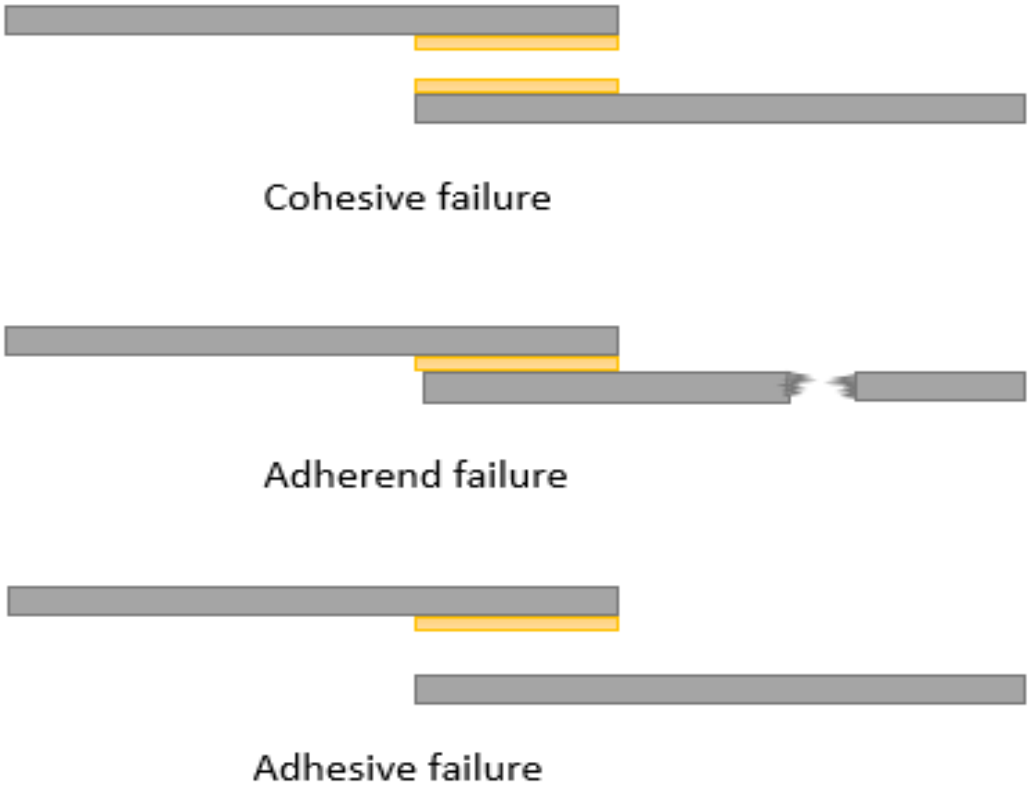

Figure 1.1 Modes of failure in adhesive bonds

excessive surface contamination of adherend surface, uncured adhesive or curing of adhesive started before application. Zero volume bonds or "kissing bonds" [14] are formed when there is no physical gap at adhesive-adherend interface, i.e. when they are in full contact, but there is little or no residual bond strength at the interface. In this study, the term "weak bond" is employed for zero-volume disbands specimens, since "kissing bond" is used as a generic term by researchers for all types of weakened bonds i.e. slip bond, partial bon, smooth bond etc.

The following criteria must be met for a bond to be defined as a weak bond [14]:

1. The strength of the weak bond must be less than 20% of the normal bond determined after a lap shear test.
2. The mode of failure must be adhesive failure (adhesive-adherend interface).
3. A normal ultrasonic inspection signal should not detect a weak bond.

A number of techniques have been used by researchers to manufacture controlled weak bonds in composite structure. Previous studies mentioned in the literature concluded that a combination of key parameters [15-24] are required to match the criteria mentioned. One proposed solution is to use solvent wiping at the adherend surface to make a weak bond [15,16]. One other well researched technique consists of applying a thin layer of mold release agent on the adherend surface before bonding. The use of release agent was either a dry layer [15, 18, 21] or a fluid [19,20,22,23]. Those techniques are relatively simple and easy to apply on composite surfaces, although the control and repeatability must be established. As highlighted by Blassa and Dilgera [24] the method of application is also important to achieve a homogeneous dry layer of release agent. Other pretreatments methods were also used to generate full strength and weak bonds [15]. Atmospheric plasma treatment on glass fiber composite specimens showed reduction in bond strength and adhesive failure [25].

An alternative technique is to modify the stoichiometric ratio of a two-component epoxy paste adhesive to influence the chemical reaction of adhesive cure proposed by Bossi et al. [15]. They also made weak bonds by making specimens with different bond line thicknesses and using varied numbers of laminate plies. McDaniel et al. [17] discussed the possibility of fabricating the weak bond specimens using controlled contamination on composite surfaces. There are several other methods which can be found in literature, like

pre-treating only a fraction of bond surface area [26], using contaminated peel ply to apply on composite surface [27], etc., to manufacture weak joints. A variety of reasons can cause weak bonds to occur, and once the structure is bonded it becomes extremely challenging to nondestructively detect the defects in an efficient and fast manner. The use of conventional diagnostics may not be useful in this case because weak bonds do not impact stiffness and only degrade the strength of the joint.

The detection and assessment of controlled weak bond specimens by nondestructive techniques have been the focus of study for many researchers to determine the characteristics of these bonds. The nondestructive evaluation techniques (NDT) employed by researchers were mostly dictated by the specific defects of their focus. Numerous evaluation techniques have been reviewed in this chapter, and some of them are further developments from conventional nondestructive methods (such as ultrasonics). Ultrasonic technique, besides being most widely used NDT, is applied in all types of materials to detect all kinds of defects. Ultrasonic testing can be sorted into two types: bulk waves and guided waves. The only difference between the two is the dimension of wavelength compared to material dimension and used according to the type of defects to be studied. Guided wave measurements with larger wavelengths are mainly used for detection of small defects in joints, such as structural health monitoring when the joint is not accessible; however, changes in adhesive bond strength cannot be evaluated by ultrasonic NDT [30].

Ultrasonic guided waves applied by Singher et al [28] show that the quality of adhesive bond affects its propagation. Brotherhood et al [29] used ultrasonic techniques to detect kissing bonds. Lamb waves are considered more reactive to interfacial defects as

compared to others to detect kissing bonds [31]. This is because specimens at different depths generate higher shear and normal stresses by lamb waves propagating under different modes. Ultrasonic waves, when passed though the nonlinear material, generate higher order harmonics. The non-linearity of the material can be used to characterize the bond strength [32,33,34]. Ries and Krautz [35] used an acousto-ultrasonic combined technique to show that stress wave factor measurement corresponds to peel strength test data. Yang et al. [36] used ultrasonic testing to observe various defects in adhesive bonds due to weak joints. Specimens with intentional poor surface preparation were used to measure damping loss factors and their response under frequency measurements. To verify the results, shear tests were conducted and compared to the model prepared. It was found that change in modal parameters were dependent upon defects of specimens. Kumar et al. [37] made weak joints prepared with varying amount of polyvinyl chloride release agent and evaluated their degradation using ultrasonic methods. Specimens were then loaded until subsequent failure to measure their mechanical strength.

1.3 Technical need and focus of current study

Heterogeneous materials are inherently dielectric in nature. Various factors contribute to the dielectric behavior of these materials, such as morphological properties and interaction of the individual components, orientation, etc. The literature shows multiple methods showing promising progress towards defect detection using nondestructive techniques; however, no concrete method provides for the effect of those defects on mechanical or electrical behavior of composite structures under interfacial defect. This creates hurdles in using adhesive bonding as a potential assembly technique. Recent research shows a new multi-physical approach to detect and follow evolution of damage in

fiber-reinforced composites under various mechanical loading [38-41]. This concept shows that damage progression in composite materials complement the changes in material state. The changes in these properties are then linked to the remaining life of the structure under loading. In this study, we want to use this concept for interfacial damage detection in adhesively bonded composite structure. This proposed concept offers that under the electric field the polarization of charge inside the weak bond is affected in thickness direction due to interfacial defect. The changes due to these interface defects can be represented in terms of dielectric variables, such as permittivity, impedance, etc., which can be related to changes in mechanical properties.

In this work, broadband dielectric spectroscopy (BbDS) is used to nondestructively identify interfacial defects, including zero defects in composite joints, both before and after adhesive bonding. Contact angle measurements were used to check the wettability of laminates whose surface was modified with induced impurities in chapter 3. Using BbDS, the effects of surface modification on its dielectric properties were then quantified. The contact angle measurements were then validated with the analysis of work of adhesion using Young's equation. Further BbDS was used to demonstrate the changes in dielectric properties due to those modification after bonding in chapter 4. Small overlap bonds were manufactured by adhesively joining carbon fiber laminates with and without surface modification and their properties were compared. Single lap joints are then studied for both mechanical and dielectric property changes due to the formation of weak interface. Several analytical models were developed in chapter 6 to understand the effect of weak interface on dielectric properties and results demonstrate that the model captures observed

experimental trend of property changes. Discussion, conclusion and future scope are included in chapter 7.

REFERENCES

1. J. R. Vinson, Adhesive Bonding of Polymer Composites, Polymer Engineering and Science, 29(19): p. 1325-31
2. V. Musaramthota, T. Pribanic, D. McDaniel and X. Zhou, Effect of Surface Contamination on Composite Bond Interity and Durability, 2013
3. Yi Hua, Ananth Ram Mahanth Kasavajhala, Linxia Gu, Elastic–plastic analysis and strength evaluation of adhesive joints in wind turbine blades, Composites Part B: Engineering, Volume 44, Issue 1, January 2013, Pages 650-656.
4. National Technical Information Services (NTIS), Literature Review of Weak Adhesive Bond Fabrication and Nondestructive Inspection for Strength Measurement, 2015
5. Baldan A. Adhesively-bonded joints and repairs in metallic alloys, polymers and composite materials: adhesives, adhesion theories and surface pretreatment. J Mater Sci 2004;39(1):1–49.
6. R. Raihan, Q. Lui, K. Reifsnider, F. Rabbi, Nano-Mechanical Foundations and Experimental Methodologies for Multiphysics Prognosis of Functional Behaviour in Heterogeneous Functional Materials, 23rd international congress of theoretical and applied mahcanics, 2014, 285-293
7. F.C. Campbell, Structural Composite Materials, Copyright 2010, ASM International.
8. Davis MJ, Bond D. Principles and practise of adhesive bonded structural joints and repairs. Int J Adhesion Adhes 1999;19(3):91–105.

9. H.J Cornille, “A high volume aluminium auto body structure; the benefits and challenges”, International body conference IBEC, Detreiot, MI, 1993; pp. 5-21.
10. J. Kinloch and C. M. Taig, J. of Adhesion, 21, p. 291, (1987).
11. Chamis CC, Murthy PLN. Simplified procedures for designing adhesively bonded composite joints. J Reinf Plast Compos 1991;10(1):29–41.
12. Banea MD, da Silva LFM. Adhesively bonded joints in composite materials: An overview. Proc Inst Mech Eng, Part L: J Mater Des Appl 2009;223(1):1–18.
13. Hoke, M.J., “Adhesive Bonding of Composites”, Abaris Training Inc.
14. Marty, N.P., Desai, N., and Andersson, J., “NDT of Kissing Bond in Aeronautical Structures,” 16th World Conference for NDT, Montreal, Canada, 2004, p. 8.
15. Bossi, R., Housen K., Walters, C.T., and Sokol, D., “Laser Bond Testing,” Materials Evaluation, Vol. 67, No. 7, 2009, pp. 818–827.
16. Barroeta-Robles, J., Cole, R., and Sands, J.M., “Development of Controlled Adhesive Bond Strength for Assessment by Advanced Non-Destructive Inspection Techniques,” SAMPE, Seattle, WA, 2010, p. 15
17. McDaniel, D., Zhou, X., and Pribanic, T., “Effect of Contamination on Composite Bond Integrity and Durability,” Technical Review Presented to Joint Advanced Materials and Structures Center of Excellence, 2012, p. 22.
18. Ecault, R., Boustie, M., Berthe, L., et al., “Development of a Laser Shock Wave Adhesion Test for the Detection of Weak Composite Bonds,” 5th International Symposium on NDT in Aerospace, Singapore, November 13–15, 2013.
19. C. Mueller-Reich, R. Wilken, und S. Kaprolat, „Bonding of plastics: Well-bonded despite residual release agents“, Adhes. SEALANTS, Bd. 3/2011, S. 36 – 41, 2011.

20. M. Wetzel, T. Rieck, und J. Holtmannspötter, „Contamination in adhesive bonding for aviation applications: Detection and effect of adhesion-limiting contaminations“, Adhes. Adhes., Nr. 2011–03, S. 29 – 33, 2011.
21. P. Marty, N. Desaï, und J. Andersson, „NDT of kissing bond in aeronautical structures“, gehalten auf der 16th World Conference of NDT Proceedings, Linköping, Sweden, 2004, S. 8.
22. M. Engholm, „A Narrowband Ultrasonic Spectroscopy Technique for the Inspection of Layered Structures“, Licence, Uppsala Universitet, Sweden, 2006.
23. J. Barroeta-Robles, R. Cole, und J. M. Sands, „Development of Controlled Adhesive Bond Strength for Assessment by Advanced Non-Destructive Inspection Techniques“, gehalten auf der SAMPE 2010, Seattle, WA, 2010, S. 15.
24. David Blassa *, Klaus Dilgera, “CFRP-Part Quality as the Result of Release Agent Application – Demoldability, Contamination Level, Bondability”.
25. Mara A, Haghani R and Al-Emrani M 2016 Improving the performance of bolted joints in composite structures using metal inserts J. Compos. Mater. 50 3001 – 18
26. Camanho P P and Lambert M 2008 A design methodology for mechanically fastened joints in laminated composite materials Compos. Sci. Technol. 66 3004 – 20
27. Hirsekorn, S., “Nonlinear Transfer of Ultrasound by Adhesive Joints—a Theoretical Description,” Ultrasonics, Vol. 39, No. 1, 2001, pp. 57–68.
28. Singher L, Segal Y, Segal E and Shamir J 1994 Considerations in bond strength evaluation by ultrasonic guided waves J. Acoust. Soc. Am. 96 2497 – 505

29. Brotherhood C J, Drinkwater B W and Dixon S 2003 The detectability of kissing bonds in adhesive joints using ultrasonic techniques Ultrasonics 41 521 – 9
30. S. Hirsekorn, A. Koka, A. Wegner, und W. Arnold, „Quality Assessment of Bond Interfaces by Nonlinear Ultrasonics Transmission“, Review of progress in Quantitative Nondestructive Evaluation, S. 1367 – 1374, 2000.
31. Internal report issued in 2002 by the Surface Treatment Department at CSM Material tekink AB., 2014.
32. Qu, J., “Ultrasonic Nondestructive Characterization of Adhesive Bonds,” Langley Research Center, NASA Technical Reports Server, Document ID: 19990046400, 1999.
33. Anastasi, F. and Roberts, M.J., “Acoustic Wave Propagation in an Adhesive Bond Model with Degrading Interfacial Layers,” MTL TR 92-63, U.S. ARMY Materials Technology Laboratory, 1992.
34. Nagy, P.B., McGowan, P., and Adler, L., “Acoustic Nonlinearities in Adhesive Joints,” Review of Progress in QNDE, Vol. 9, 1991, pp. 1685–1692.
35. dos Reis, H.L.M., and Krautz, H.E., “Nondestructive Evaluation of Adhesive Bond Strength Using the Stress Wave Factor Technique,” Glenn Research Center, NASA Technical Reports Server, Document ID: 19870044926, 1986.
36. Shuo Yang, Lan Gu, and Ronald F Gibson. Nondestructive detection of weak joints in adhesively bonded composite structures. *Composite Structures*, 51(1):63{71, 2001

37. RL Vijaya Kumar, MR Bhat, and CRL Murthy. Some studies on evaluation of degradation in composite adhesive joints using ultrasonic techniques. *Ultrasonics*, 53(6):1150{1162, 2013.
38. Fazzino, P.D., K.L. Reifsnider, and P. Majumdar, Impedance spectroscopy for progressive damage analysis in woven composites. Composites Science and Technology, 2009. 69(11-12): p.2008-14.
39. Reifsnider, K.L., et al., Material state changes as a basis for prognosis in aeronautical structures. Aeronautical Journal, 2009. 113(1150): p. 789-798.
40. Fazzino, P. and K. Reifsnider, Electrochemical impedance spectroscopy detection of damage in out of plane fatigued fiber reinforced composite materials. Applied Composite Materials, 2008. 15(3): p. 127-138.
41. Reifsnider, K. and P. Majumdar, Material state change relationships to fracture path development for large-strain fatigue of composite materials. Mechanics of Composite Materials, 2011. 47(1): p. 1-10

CHAPTER 2

BACKGROUND ON EXPERIMENTAL METHODS

2.1 Measurement of adhesion characteristics

Contact angles measurements are used as an indicator of surface wettability of solid surface under examination and to enable the determination of surface free energy. It is defined as an angle formed by the soli-liquid interface of a sessile liquid drop. Contact angle are considered as a standard surface quality measurements technique among various methods available. It is based on fundamental understanding that since adhesives are liquids, the way any liquid adheres to a bonding surface, predicts the way adhesive adhere. Contact angle will be small if the surface preparation is good and liquid spreads on surface, while a large contact angle indicates poor surface preparation and liquid beads on the surface. Thomas young [1] defined the mechanical equilibrium of liquid drop on ideal solid surfaces under the action of three interfacial tensions:

$$\gamma_{SV} = \gamma_{SL} + \gamma_{LV}\, cos\theta \quad ----------(1)$$

Several contact measurement methods are available in literature, based upon the solid surface and type of application. Bigelow et at. [2] used a telescope-goniometer to measure contact angle of polished surfaces. Leja and Poling [3] made some modification to capture drop profile and added the camera in telescope-goniometer. Further modification was done controlling the fluid flow by adding a motor driven syringe in instrument [4]. The goniometer methods also suffer from some serious limitations, like measurement of small contact angle (below 20°), dependence of contact angle on the drop size [5,6] etc.

2.2 Visualization

In order to examine the microstructural changes in a composite material, Image visualization is important as we are able to observe these changes directly and accurately. When 2D analysis is required, many orthodox methods are readily available, such as an optical microscope, scanning and transmission electron microscopes (SEM and TEM). In the case of SEM, a beam of electrons is focused on the sample and used to scan its surface, When the beam of electrons make contact with the sample surface, the surfaces atoms interact with the surface atoms to give off a variety of signals and beams which can be used to deduce useful information about the surfaces tomography and constitution. A Raster patterns scan along with a combination of the coordinates from the electron source and detected reflected signal data is used in order to produce the final scan. Similarly, in the case of TEM, electron is used, but in this situation, the beam is made to pass through the sample, which interact with the atoms of the sample along their path. In this case, the scanned sample needs to be very thin in order to facilitate efficient transmission of electrons. The reaction signals are then used to construct the image which can then be analyzed.

To fully analyze the micro structure inside of a composite structure, traditional surface visual inspections are not adequate. Thus, higher level of inspection is required. Techniques such as X- Rays, acoustic scanning and ultra-sonic scanning have proven to be effective techniques. In the case of Ultrasonic inspection, very low wavelength waves are transmitted into a sample and the change in the waves are used to estimate the internal structure. This method is popular in scanning metallic structures but not optimal for composites due to low resolution of output in their case. Unlike ultrasonic scanning,

Acoustic monitoring is used to record audible signals produced during the formation of damage under load in real time and the data set is used to analyze the damage progression. For example, in the case of an Aircraft, a large number of acoustic sensors can be mounted near an area of heavy load such as the landing gear and the sound produced during damage can be recorded in real time and its location can be triangulated using the time to reach each of the sensors.

Finally, the method of 3D X-ray Spectroscopy is an advanced visualization technique, which uses x-ray waves which originate at the X-ray source, pass through the sample of interest and are finally picked up by the receiver. The X-rays change in intensity depending on the density and other factors of the sample as they pass through it. This data is then used to construct CTs (Computed topographies) which are the computed to create a 3D data image. This method is highly advantageous in analyzing the microstructure of composites as it can detect micron sized defects while being completely nondestructive. Some advanced instruments are even capable of maintaining high image resolution even when operating at relatively large distances, thus being able to scan even large samples.

Table 2.1 Resolution range and field of view on a MicroXCT-400 3D X-ray Microscope at different settings.

Magnification Level	**Resolution Range (μm)**	**3D Field of View (mm)**
1X	9 – 22	4 - 15
4X	5 - 6	2.4 – 6
10X	1.5	2 – 2.7

REFERENCES

1. T. Young, Philos. Trans. R. Soc. Lond. 95, 65 (1805)
2. J. Leja, G.W. Poling, On the interpretation of contact angle, in Proceedings of the 5th Mineral
3. Processing Congress (IMM, London, 1960), p. 325
4. R.W. Smithwich, J. Colloid Interface Sci. 123, 482 (1988)
5. D.Y. Kwok, R. Lin, M. Mui, A.W. Neumann, Colloids Surf. A 116, 63 (1996)
6. S. Brandon, N. Haimovich, E. Yeger, A. Marmur, J. Colloid Interface Sci. 263, 237 (2003)
7. P. Letellier, A. Mayaffre, M. Turmine, J. Colloid Interface Sci. 314, 604 (2007)

CHAPTER 3

EFFECT OF SURFACE MODIFICATION

Carbon fiber composites are high-strength, light and custom-made materials and are therefore in highest demands, e.g. in aircraft construction and for sports apparatus. The joining of the composite parts, where adhesives are frequently used, requires appropriate pretreatment. There are several successive actions that are needed to prepare an adhesive joint. Clean adhered joint surface is important so that the surface can be on high energy state to achieve a good bond. During manufacturing of CFRP laminates surface impurities like mold agent, water, and organic debris may prevent proper wetting and adhesive spreading on the joint surface. This subsequently hinders adhesion [10]. Because of bad adhesion of composites parts due to surface impurities, the bond is weakened and fails at significantly lower level. There are several surface pre-treatments like application of peel ply [4], mechanical treatments [5, 6] or physical treatment [7, 8] that can avoid the effects of impurities.

There is a need for a non-destructive method to evaluate the adherend surface quality before bonding. Contact angle and wetting measurements are standard surface analytical tools for benchmarking the surface quality [11]. The measure for the wettability of a solid with a liquid is the contact angle between the two phases: the larger the contact angle, the smaller the wetting. Figure 3.1 shows contact angles of different surfaces: a large contact angle is detected when the liquid beads on the surface ($\theta>90$) which indicate poor wetting, and a small contact angle is recorded when liquid spreads on the surface ($\theta<90°$)

which is favorable for wetting. Moreover, complete wetting occurs as the droplet is flat (θ=0°).

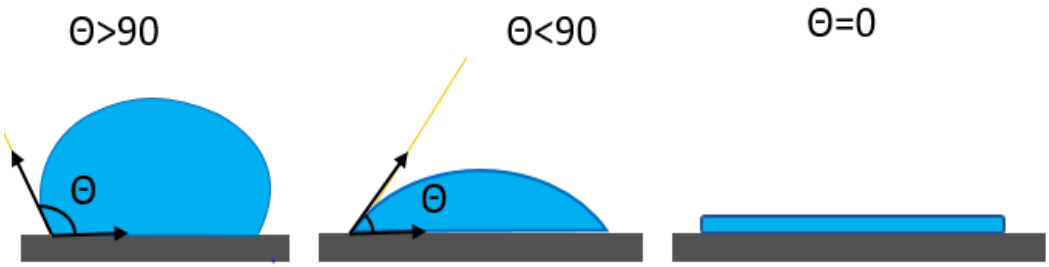

Figure 3.1 Contact angles of different kind of surfaces.

The objective of this chapter is to use contact angle measurements to determine the surface quality of laminate surfaces that have been modified with different impurities. The effect of surface modification on dielectric properties are quantified using broadband dielectric spectroscopy (BbDS) technique.

3.1 Quantification of surface modification

In this study, contact angle is measured on modified surface of 1/8" mm quasi isotropic carbon fiber composite (CFRP) laminate under influence of mold release agent (RA) and surface contamination to investigate the bonding ability of laminate surface. The use of release agent for manufacturing of CFRP is unavoidable. Because of demolding after curing [2], various types of RAs are studied to determine their effect on bond quality and surface appearance.

3.1.1 Specimen preparation

In this study, four group of specimens were prepared with different type of surface conditioning. 1" X 1" square specimens are used in this study were cut from 2' X 1' premade 1/8" quasi isotropic CFRP laminate by water cooled circular tile saw. Sanding

was done by 600 grit sandpapers to remove the glossy finish of laminate and all the other impurities like dirt, grease, or other contaminants were removed by wiping the surface with acetone. Dip coating and wiping leads to much more homogeneous surfaces without agglomeration [3] compared to spraying. Figure 3.1 shows the images surface after preparation. Following are descriptions of the four specimens:

1. Specimen A – Laminate surface was prepared without any sanding or solvent wiping.
2. Specimen B – Laminate surface was prepared by sanding and solvent wiping the surface as recommended for bonding surface preparation.
3. Specimen C – Laminate surface was sanded, solvent wiped and then dip wiped three times by water based fibrelease RA (FRA).
4. Specimen D – Laminate surface was sanded, solvent wiped and a silicon based release agent (Si RA) was sprayed three times.

3.1.2 Test liquid

In this study, we used two testing liquids: distilled water and epoxy resin (Fiber Glast 2000). Since the water based release agent (FRA) used in the study is hygroscopic [1], epoxy is used to compliment the measurement with water.

3.1.3 Instrument and visualization method

A standard 1 oz. calibrated glass dropper (Figure 3.2) is used to drop a controlled amount of fluid for this experiment. During the measurement, the specimens were placed on a flat surface and liquids were dropped from very close distance to prevent drop splitting. The camera was placed perpendicular to the specimen surface to get accurate

angles, and burst mode was used to obtain pictures for this experiment. Onscreenprotractor software was used to measure the contact angle from images.

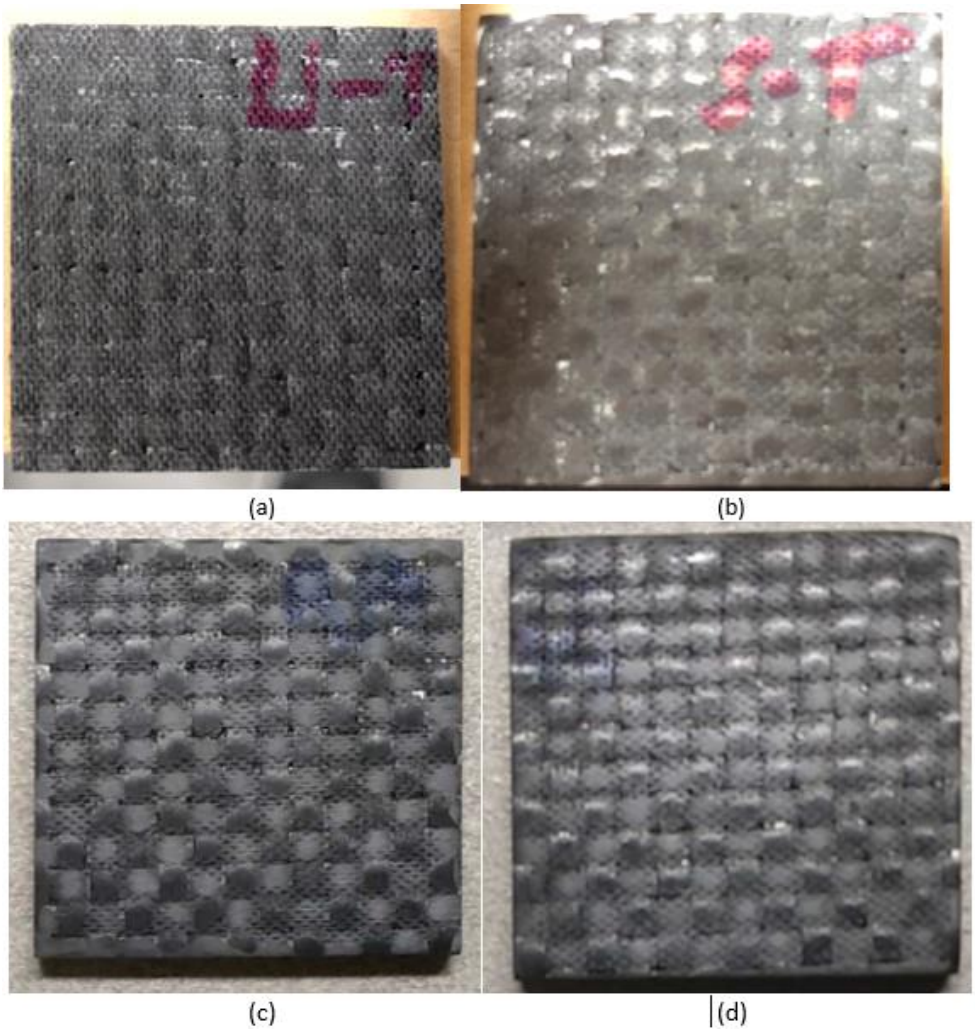

Figure 3.2 laminate surfaces after Release agent application (a) unsanded laminate, (b) sanded laminate, (c) laminate with Fibrelease RA, (d) laminate with Silicon based RA.

3.1.4 Test procedure and results

3.1.4.1 Water as test liquid

Table 3.1. shows the contact angle measured for with different surface impurities specimens with water as test liquid:

Table 3.1. Wettability (degrees)

Specimen A	31
Specimen B	38
Specimen C	113
Specimen D	110

The result shows that specimens with RA have contact angles more than 95 degrees, which qualify them as poor bonding surfaces. On the other hand, contact angle of 31° for sanded specimen indicated a reasonably good surface to bond. Figure 3.3 shows pictures used to measure the contact angle.

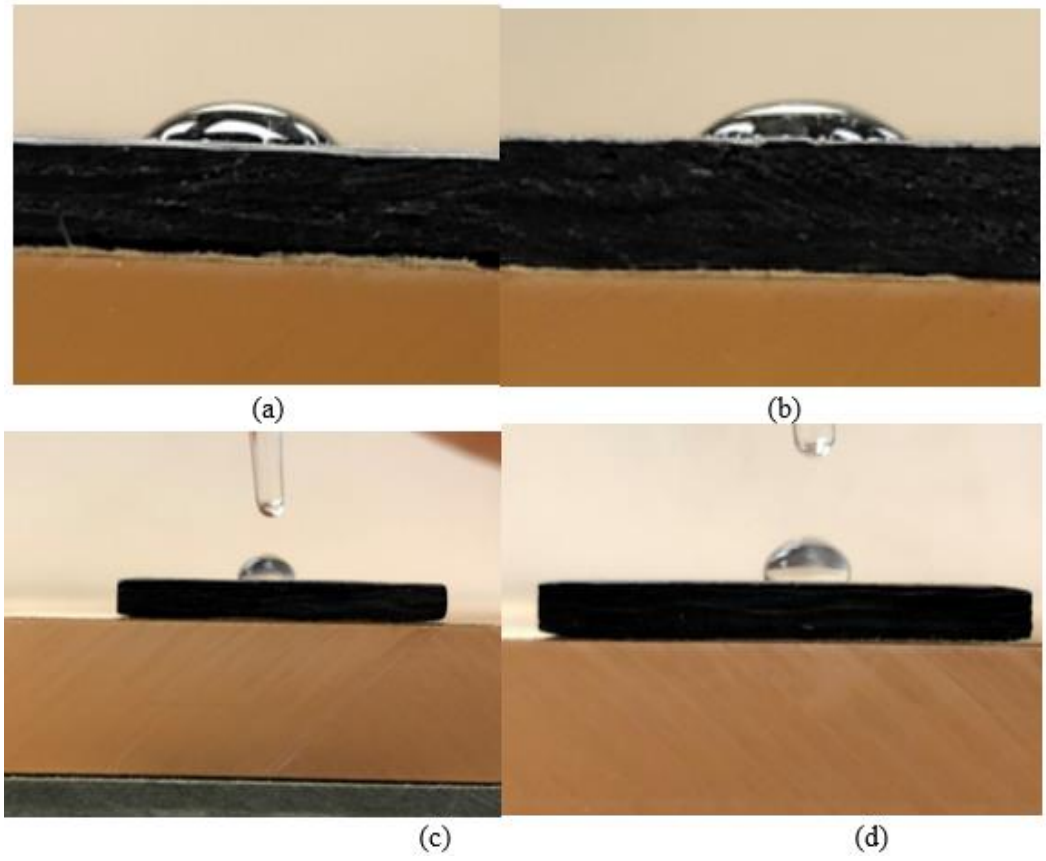

Figure 3.3 Contact angle pictures (a) specimen A, (b) specimen B, (c) specimen C, (d) specimen D

During the investigations, it was found that contact angle of laminate surface with FRA was changing quickly as presented in other research [1].

Figure 3.4 Images of specimen C taken at different time (a) Right after drop touch the laminate, (b) 5 mins later

3.1.4.2 Epoxy resin as test liquid

As epoxy has higher viscosity than water, the contact angle was slightly higher for non-RA surfaces. Table 3.2 shows the contact angle measurement with epoxy resin as test liquid:

Table 3.2. Wettability (degrees)

Specimen A	56
Specimen B	48
Specimen C	117
Specimen D	110

The contact angle of 44° for epoxy was obtained from an abraded and cleaned surface, again demonstrating that the surface is reasonably clean and ready for adhesive bonding. Figure 3.5 shows the different images acquired for calculation.

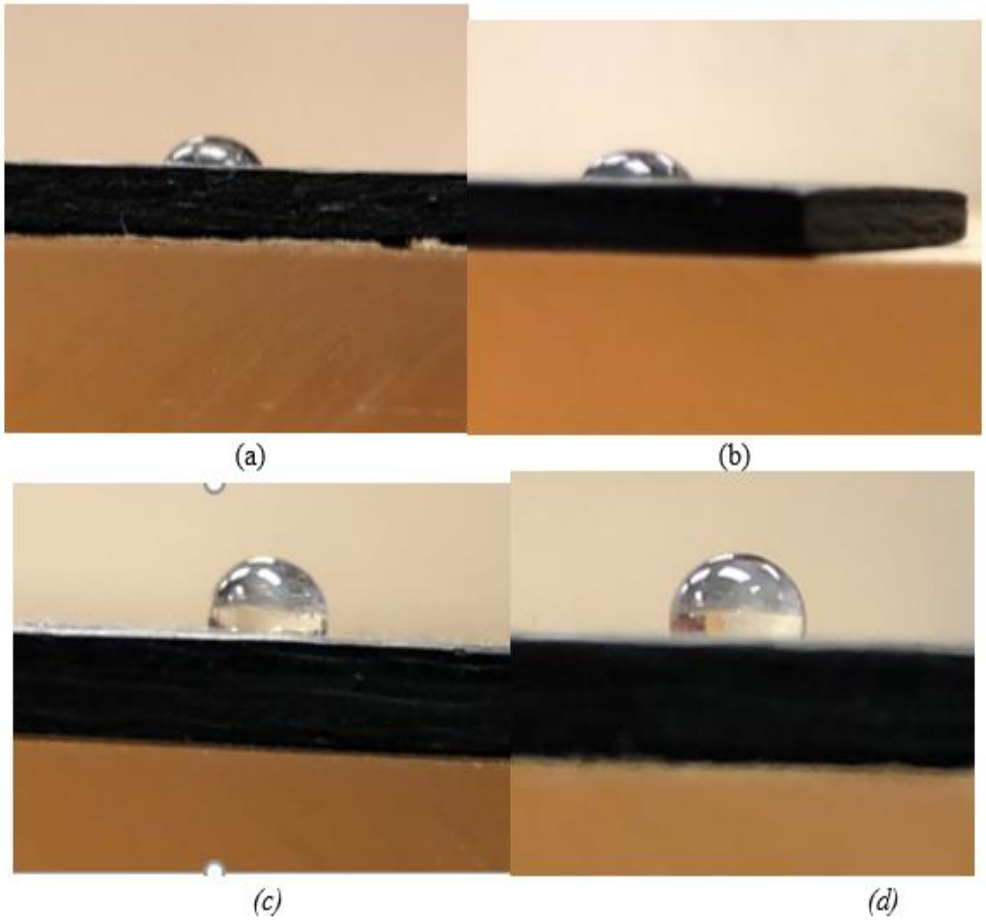

Figure 3.5. Contact angle pictures (a) specimen A, (b) specimen B, (c) specimen C, (d) specimen D

3.2 Analysis of surface contact angle and surface energy

Adhesive bonding involves adhesive and adherend. From typical failure analysis, it is observed that failure of adhesive or adherend is called cohesion mode and is considered acceptable, while failure at the interface or interphase is called adhesion mode and is a sign of a weak bonding strength. In other words, cohesion is due to strong intermolecular attractions between like-molecules/atoms and is often reported as the cohesive strength (of

adhesive for example). There are different bonding mechanisms well described in the literature such as primary covalent bonding, secondary bond (dispersion forces between atoms), molecular inter-locking, inter-diffusion, ionic bond etc. Two important surface parameters contribute significantly to above adhesion mechanisms: surface energy and roughness. These parameters are directly related to work of adhesion (Wadh) and then to strain energy release rate (G). This implies that surface preparation can significantly control and define the quality (strength or fracture properties) of the bond achieved.

The first basic requirement for adhesion is that the adhesive must wet the surface and penetrate the roughness as shown in figure 3.6.

Young-Dupre equation relates surface energy with contact angle and creates a measurable pathway towards changing surface energy of adherend surface and control work of adhesion.

$$\gamma_{SV} = \gamma_{SL} + \gamma_{LV}\, cos\theta = \gamma_{SL} + \gamma_L\, cos\theta \quad ---------- (1)$$

$$Work\ of\ Adhesion, W_{adh} = \gamma_{SV} + \gamma_{LV} - \gamma_{SL} = \gamma_S + \gamma_L - \gamma_{SL} = \gamma_{LV}\,(1 + cos\theta) - (2)$$

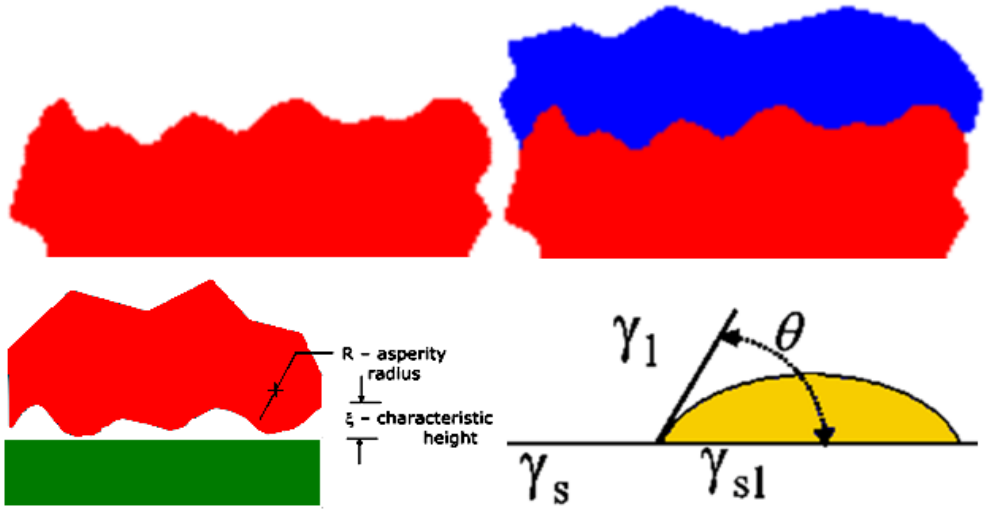

Figure 3.6 Adhesive ability to wet rough surface

Table 3.3 Estimation of bond quality in terms of work of adhesion

		Surface energy, γ_{LV} mJ/m^2	Contact angle, θ degree	Work of adhesion
Base laminate	water	72	38	128.73
Base+water based RA	water	72	113	43.86
Base+Si RA	water	72	110	47.37
Base laminate	epoxy	42-47	48	71.77
Base+water based RA	epoxy	42-47	117	23.47
Base+Si RA	epoxy	42-47	110	28.29

The contact angle measurements by Young's equation assume a smooth surface and can be further modified to account for surface roughness by using the well-known Wenzel equation:

$$roughness\ ratio, r\ (>1) = \frac{contact\ angle\ of\ rough\ (Wenzel)\ surface,\ cos\theta_2}{contact\ angle\ of\ smooth\ (Young)\ surface,\ cos\theta_1}$$

The roughness ratio is 1 for smooth surface and greater than 1 for rough surface. This equation predicts that for contact angles less than 90°, wetting is increased by surface roughness, but decreased for non-wetting materials with contact angles greater than 90°.

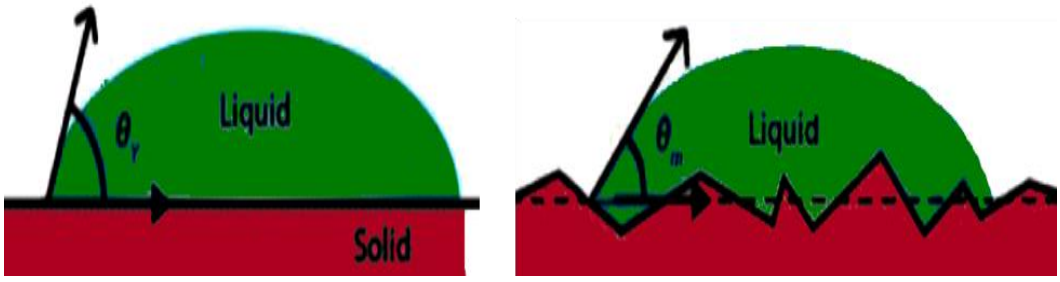

Figure 3.7 Smooth (left) and rough (right) surfaces

Table 3.4 Effect of roughness on contact angle

Surface modification type	Liquid used for contact test	Contact angle, θ (degrees)	Approximate roughness, r by Wenzel equation
Un-sanded carbon/epoxy	epoxy	56	1.196
Additional light sanding	epoxy	48	

This shows that there is roughness in the surface. Researchers (Curtis Holmes, On the Relation between Surface Tension and Dielectric Constant, Journal of the American Chemical Society 195:4 1973) have now shown that there is direct correlation between surface energy (function of surface properties and surface roughness) and dielectric constant. In fact, they showed an empirical relationship of the following form with constants a, b and functional form of dielectric constant.

$$\gamma = a\,F(\varepsilon_0) + b \quad ---------(3)$$

This provides us the basis to justify that the observed dielectric property changes are essentially due to changes in true change in chemical bonding characteristics, roughness and surface energy. A successful creation of weak interface is demonstrated by dielectric property change data in this thesis work.

3.3 Dielectric property changes due to surface modification

In the previous section, various types of surface modification of CFRP laminates were quantified by performing wettability tests. Here, we will try to capture the surface modifications through broadband dielectric spectroscopy (BbDS). BbDS is used to scan the laminate before and after modifying the surface to capture and relate the changes in dielectric properties to the surface modification.

3.3.1 Dielectric measurement procedure

Novocontrol^{TM} America Inc. supplied the BbDS unit (figure 3.8) used in this experiment. The system also consists of alpha analyzer for all the complex dielectric properties measurements against the frequency. The software used with this device is WinDETA, which measures minor changes in material properties as it is subject to a periodic electrical field to characterize its molecular kinetics. The complex dielectric function $\varepsilon*$ depends on the temperature and angular frequency ($\omega=2\pi f$). This measurement will help us relate the changes in dielectric properties (such as permittivity) to the laminate surface preparation. The system can do wide range of frequency analysis, from 3 µHz to 20 MHz and impedance range from 10^{-3} to 10^{15} Ω at ambient to 1200°C.

In this study, broadband dielectric spectroscopy (BbDS) is used to determine the changes in material properties caused by surface modification of laminates. Dielectric measurement of all the specimens were carried out before and after applying the release agent (FRA and Si RA) on the specimen surface at room temperature. Copper electrodes are made similar to specimen's size, i.e. 1" X 1", and attached to a PTFE Teflon block of 2" X 2" and are connected to BbDS unit via alpha analyzed. The tests were performed with electrode assembly enclosed in the faraday cage (figure 3.8) to cancel any electromagnetic noise with electrodes on either side of the specimen during scanning. Toggle clamp is used to ensure proper contact electrodes and specimen during scanning.

3.3.2 Specimen preparation

In this study, we will study two cases of surface modification. 1" X 1" specimens were cut from premade 1/8" quasi isotropic CFRP laminate, then sanded, solvent wiped and scanned in BbDS. After scanning, one specimen is dip wiped three times with FRA

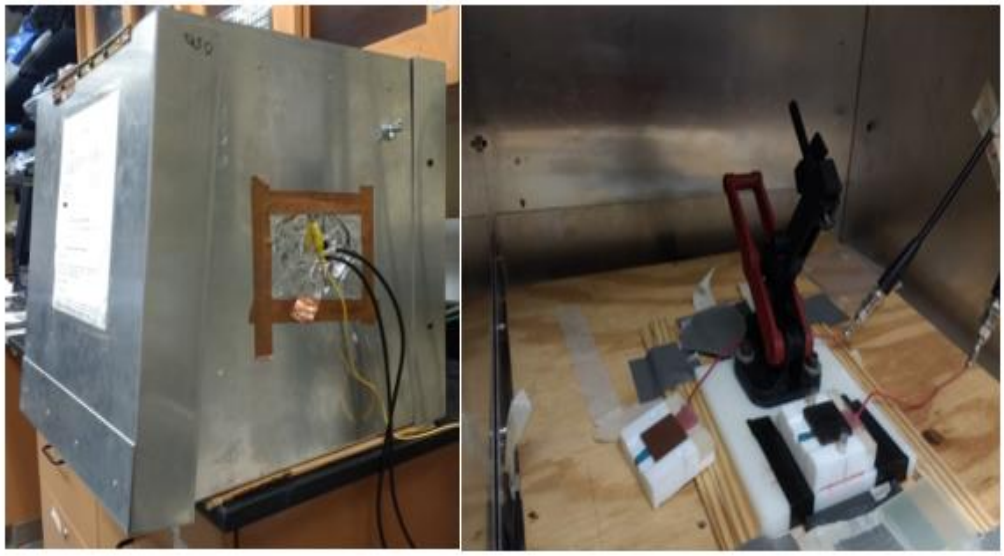

Figure 3.8. BbDS faraday cage (left) and toggle clamp with electrode (right)

and the other specimen is sprayed three times with Si RA and scanned in BbDS again to study the variation in dielectric properties.

3.3.3 Results and discussion

3.2.3.1 Surface modification with Fibrelease (FRA)

We have taken bulk BbDS measurements of specimen before and after application of FRA and looked at change in dielectric properties to capture effect of laminate surface modification.

As seen from figure 3.9, there is a significant change in imaginary permittivity at lower frequency. Figure 3.10 demonstrates that Impedance is more sensitive to surface modifications. This finding can significantly enhance our understanding of how surface modifiers can affect dielectric properties

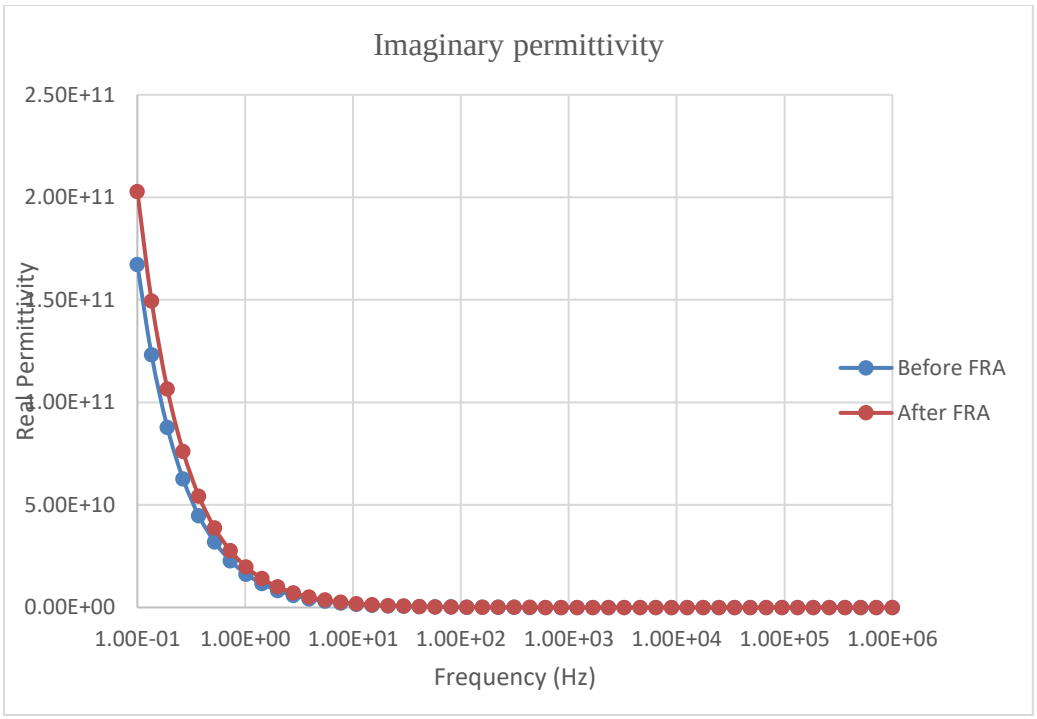

Figure 3.9. Imaginary Permittivity as a function of frequency before and after applying FRA on laminate surface

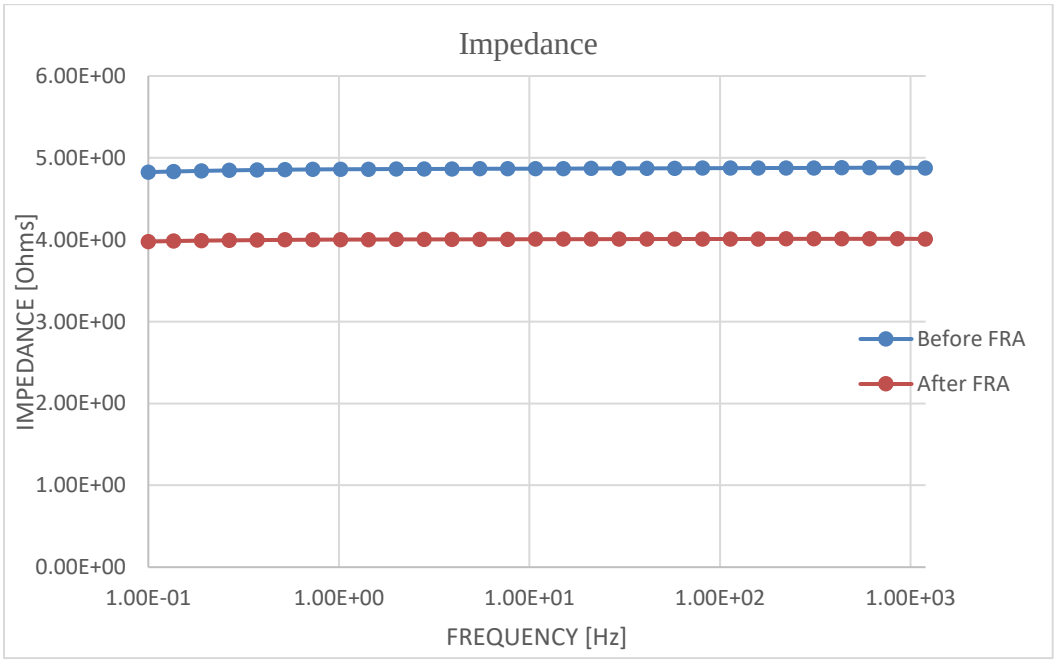

Figure 3.10. Change in AC impedance function of frequency before and after applying FRA on laminate surface

3.2.3.1 Surface modification with Silicon release agent

Here are the changes in imaginary permittivity before and after applying the silicon based release agent (Si RA) in figure 3.11.

It is clear graph above that imaginary permittivity is more sensitive at lower frequencies. There is hardly any change in imaginary part. We also compare the impedance here.

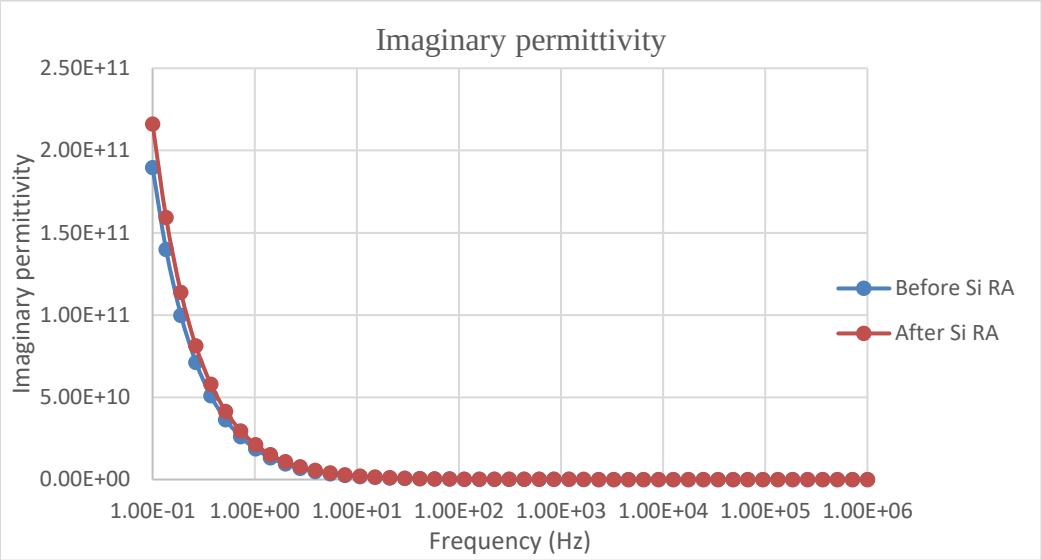

Figure 3.11. Change in imaginary permittivity as a function of frequency before and after applying FRA on laminate surface

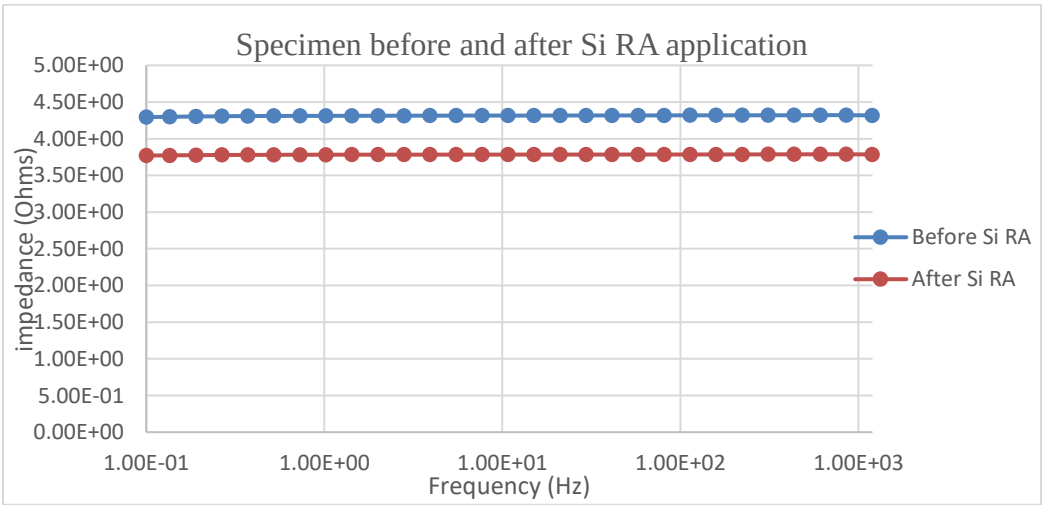

Figure 3.12 Change in AC impedance function of frequency before and after applying FRA on laminate surface

For better comparison, we normalized and plotted the dielectric properties (at set frequency of 0.1 Hz) of the specimens with and without surface modification.

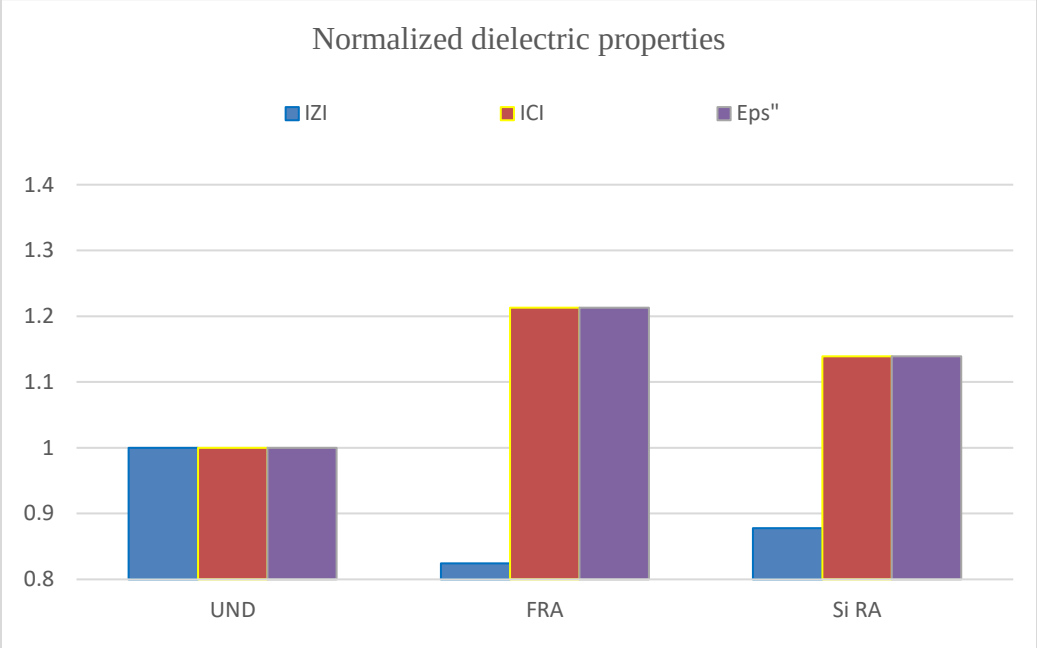

Figure 3.13 Change in dielectric properties as a function of frequency with different surface defects

3.4 Summary and observation

Wettability of composite laminate surfaces under various modifications was measured and verified using analytical methods. Broadband dielectric spectroscopy (BbDS) was used to scan laminates before and after modifications were done on its surface. Results prove that BbDS can capture the modifications by change in the dielectric properties of laminates because of those modifications.

REFERENCES

1. CRITCHLOW, G.W. ... et al, 2006. A review and comparative study of release coatings for optimised abhesion in resin transfer moulding applications. International Journal of Adhesion and Adhesives, 26 (8), p.577-599.
2. Rosato DV, Rosato DV. Reinforced Plastics Handbook. 3rd ed. Oxford: Elsevier; 2005
3. David Blassa *, Klaus Dilgera, "CFRP-Part Quality as the Result of Release Agent Application – Demoldability, Contamination Level, Bondability".
4. Kanerva M, Saarela O. The peel ply surface treatment for adhesive bonding of composites: A review. Int J Adhes Adhes 2013; 43:60–9.
5. Hu NS, Zhang LC. Some observations in grinding unidirectional carbon fibre-reinforced plastics. J Mater Des Appl 2004; 152:333–8.
6. Ashcroft IA, Hughes DJ, Shaw SJ. Adhesive bonding of fibre reinforced polymer composite materials. Assembly Autom 2000; 20:150–61.
7. Holtmannspötter J, Czarnecki JV, Wetzel M, Dolderer D, Eisenschink C. The Use of Peel Ply as a Method to Create Reproduceable But Contaminated Surfaces for Structural Adhesive Bonding of Carbon Fiber Reinforced Plastics. J Adhes 2013; 89:96–110.
8. Fischer F, Kreling S, Jäschke P, Frauenhofer M, Kracht D, Dilger K. Laser Surface Pre-Treatment of CFRP for Adhesive Bonding in Consideration of the Absorption Behaviour. J Adhes 2012; 88:350–63
9. D.J.Gordon and J.A.Colquhoun., Adhesives Age, June 1976.

10. Parker BM, Waghorne RM. Surface pretreatment of carbon fibrereinforced composites for adhesive bonding. Composites 1982; 13:280–8.
11. Berg, J. C. Wettability; Surfactant Science Series 149; Marcel-Dekker: New York, 1993.

CHAPTER 4

INTERFACIAL DEFECT AND PROPERTIES OF BONDED LAMINATES

4.1 Different Interfacial defects

The use of adhesive bonding of composites is gaining popularity over conventional mechanical fastening, especially in aerospace industry. There is rising demand for development of appropriate nondestructive inspection methods to determine the durability of the adhesive bond strength, to continue the safe use of bonded structure. In the previous chapter, we replicated common surface impurities on CFRP laminate and evaluated those using nondestructive methods. We used contact angle measurement to quantify the type of surface defects and related those defects with the dielectric properties using broadband dielectric spectroscopy technique. Contact angle measurements are an accurate and efficient way to check the bond surfaces, but there is an urgent need to develop an efficient nondestructive testing method to predict defects after the surfaces are adhesively boded.

In this work, “good” and “weak” adhesively bonded overlap joints were prepared. Weak joints are controlled, reduced-strength adhesive joints with diverse interfacial defects. One batch of specimens were manufactured with surface defect and the others with volume defect. BbDS measurement are taken in all the specimen to determine dielectric properties change as a function of defect type and or size and compared to the undamaged specimens.

4.1.1 Adhesive preparation

All the adhesive samples are made by high strength structural adhesive, commercially manufactured by Fiber Glast 1101 and comes in in 2 parts (part A and part B). Part A is adhesive whereas part B is a hardener to cure part A. The mix ratio is 1:1 by weight or volume; we did the mixing by weight in this study. A standard weighing scale with minimum weighing capacity of 1 gms was used to measure the weight while mixing. To maintain the consistent bond quality for all the joints specimens, the same weight of part A and part B was used every time, i.e. 100 gms of each part A and part B is mixed every time the specimens were made. Speedmixer^{TM} (figure 4.1) by FlackTek Inc. was used to mix both the part adhesive. Speedmixer uses dual asymmetric centrifugal mixing technology to mix fluid at very high speed (800-2500 rpm), provides bubble-free mixing and homogenizes the mixture. For our study, we mixed the adhesive in speedmixer at 1500 rpm for 3 mins. Since the mixture is viscous, plastic sponge is used to spread it on the laminates. A custom-made clamp fixture was made to hold the sample while the adhesive was curing. The joints were left to cure at room temperature for 24 hours under constant pressure on overlap area on the fixture as recommended by the manufacturer.

4.1.2 Specimen preparation

4.1.2.1 Specimen with volume defects

Two group of specimens were made to study the effect of volume defect or debond in overlap joints, manufactured by adhesively joining 1/8" quasi isotropic carbon fiber reinforced laminate (figure 4.2).

1. One group was made with inclusion of Teflon tape at one adhesive-adherend interface. Six different specimens were manufactured with 0% (undamaged) to

Figure 4.1 SpeedMixer

75% (3/4” X 3/4" surface area on 1” X 1” laminate) of surface area of laminate covered with Teflon. The teflon tape used has thickness 0.0032”-0.0038” and is chemically inert.

1. The second group was made with release film at one adhesive-adherend interface. Specimens were made with 0% to 60% of laminate surface area covered with release film. The release film used is 0.002” thick.

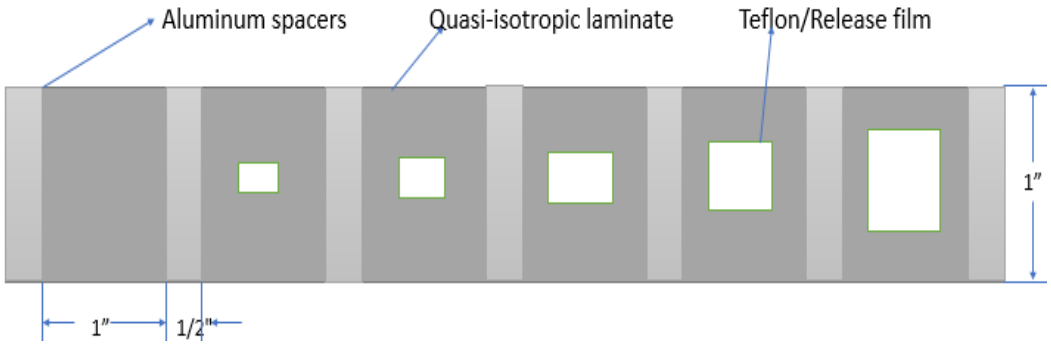

(a)

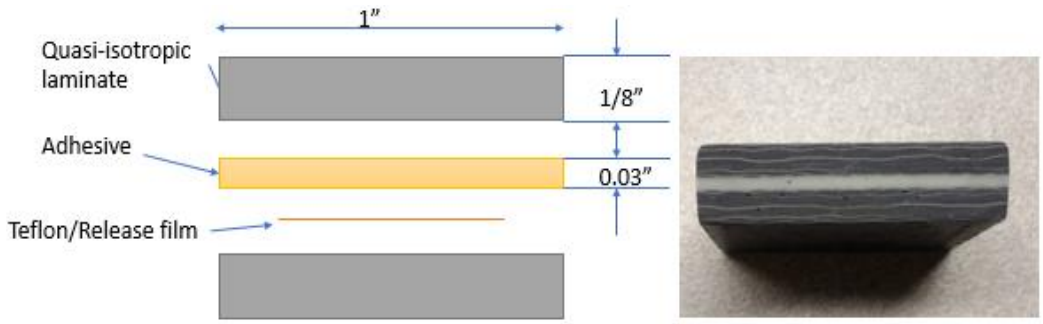

(b)

Figure 4.2. Schematic of overlap joint preparation with Teflon/release film

Specimens with teflon and release film were made in following steps:

1. Two 9.5” X 1” pieces were cut out from the laminate, sanded the bond side in both, cleaned with acetone to be bonded with adhesive.
2. Spacers of aluminum ½” wide were used to maintain 0.03” thickness of the joint. The spacers were glued to the laminate at 1” spacing as shown in figure 4.3.
3. Teflon or release film were cut and placed on one laminate with spacers according to the percentage of surface area. Place the laminate on clamp fixture.
4. Prepare the adhesive mix as directed in section above, pour on laminate surface with spacers on it.
5. Position the second laminate on top of this laminate and clamp the fixture, the extra adhesive will squeeze out automatically. Cure for 24 hours at room temperature
6. Cut out the area with spacers to get 1” X 1” overlap specimens, polish with 600 grits paper and clean with acetone to make it ready for scanning.

4.1.2.3 Specimen with surface defects

To replicate weak adhesive bond with surface defects, one interface of overlap joint was modified. Four different groups of specimens were made with 3 mm quasi isotropic carbon fiber reinforced laminate and their interfacial polarization studied.

The differentiating feature between these specimens was type of surface modification done on adhered surface in the bonding interface.

1. Specimen-1 were made without any modification, to replicate “good” bond.
2. Specimen-2 had their surface modified with fibrelease mold release agent.
3. Specimen-3 were modified with Silicon based release agent
4. Specimen-4 had their surface modified with wax.

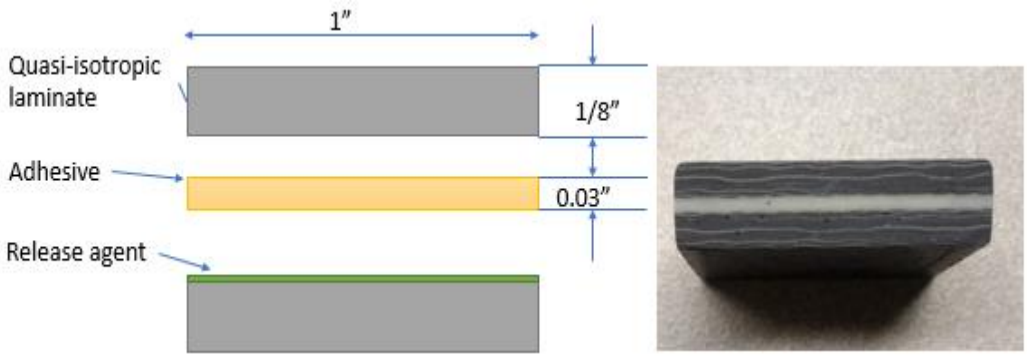

Figure 4.3. Adhesively bonded overlap joint (right) and schematic of same (left)

To make these specimens, steps provided in above section were followed. The only difference was, instead of teflon tape or release film, three coatings of release agent (in case of fibrelease and silicon release agent) and wax were applied all over on the bonding surface of one of the laminates. The application of fibrelease and silicon release agent was done as discussed in the previous chapter. Wax was applied uniformly on the laminate surface.

4.2 Dielectric property changes due to surface modifications

Dielectric measurement was done using the same Novocontrol equipment described in chapter 3, the range of frequency for collecting data was 0.1 Hz to 1kHz.

4.2.1 Effect of surface defects on dielectric properties

BbDS measurements have been taken of overlap joints with various interfacial defects. These results capture change in real permittivity due to various interfacial defects. The graphs prove that BbDS can capture the type of defects. We also observed the change in values was significantly higher at low frequency, especially when we go below 1 Hz. Capacity values are plotted vs frequency:

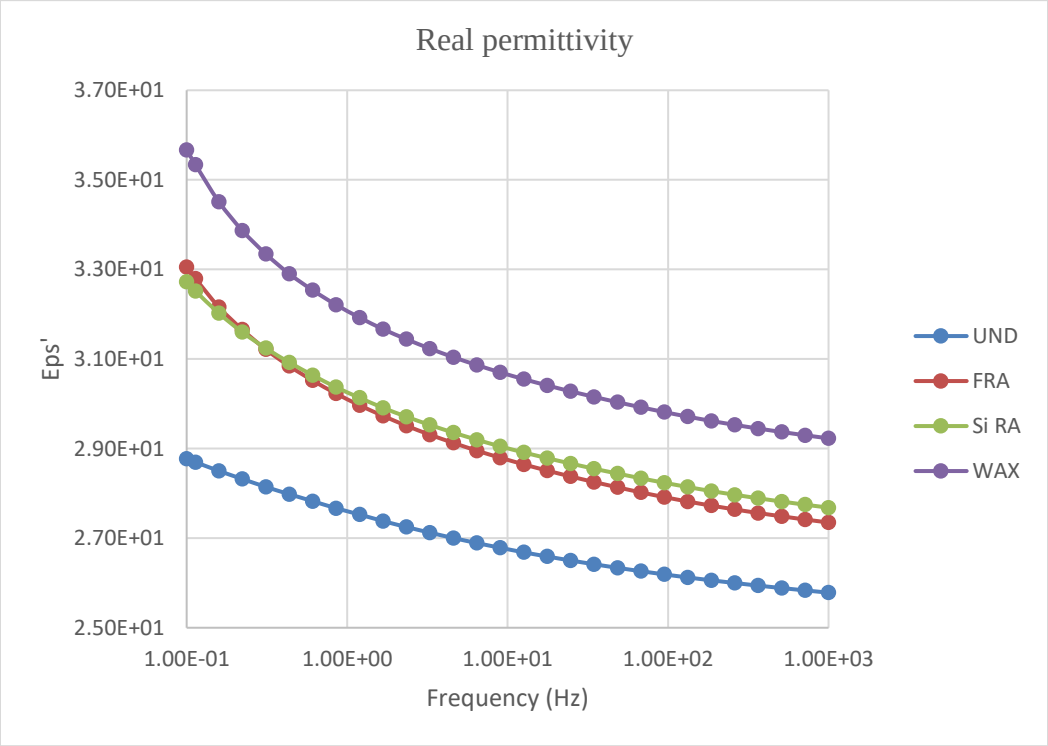

Figure 4.4. Change in permittivity as a function of frequency of different surface defects

Like permittivity plots, capacity values also change more substantially at low frequency. To understand the changes in properties better, we normalized the impedance values and plotted at 0.1 Hz.

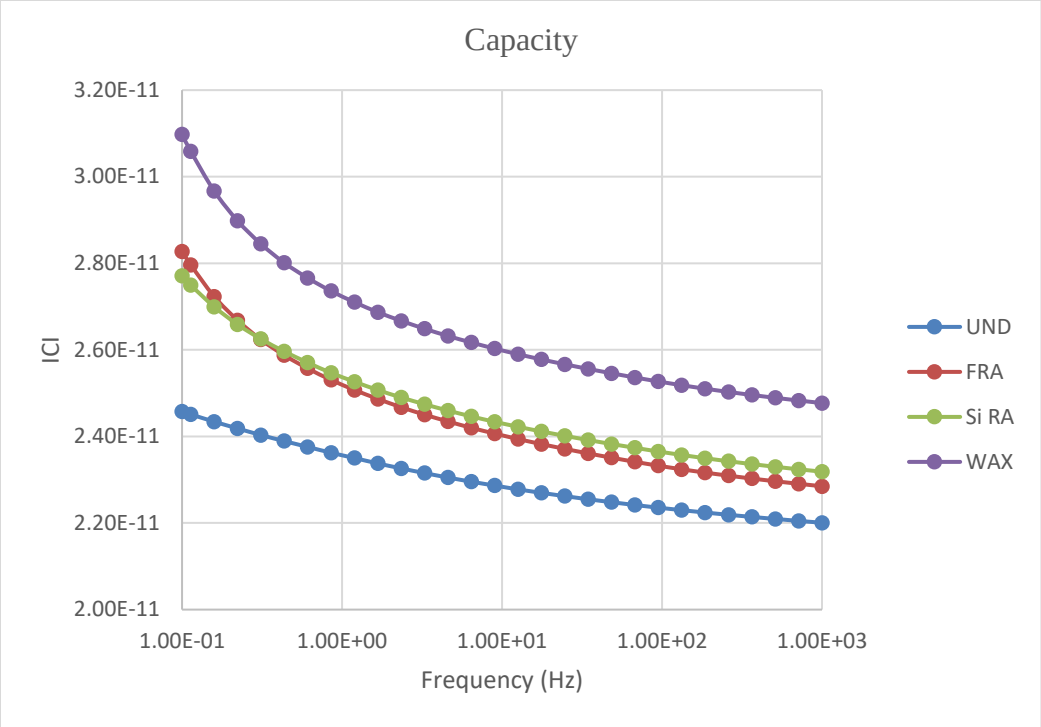

Figure 4.5 Change in capacity as a function of frequency of different surface defects

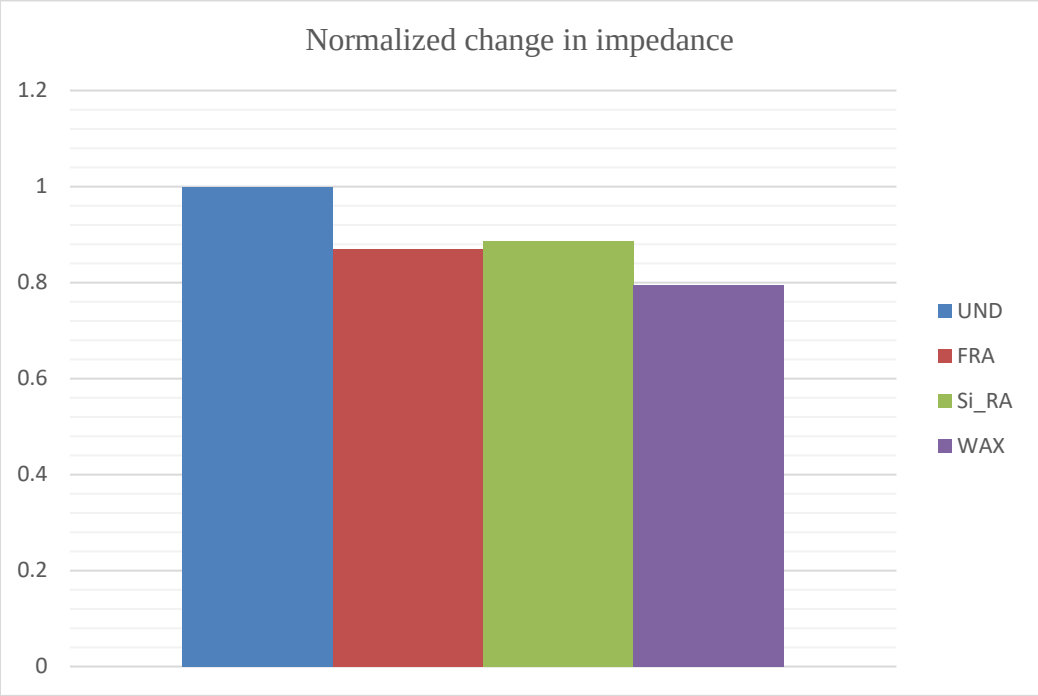

Figure 4.6 Change in dielectric properties as a function of frequency with different surface defects

This method has great potential for nondestructive evaluation of bonded composite joints for detecting defects. The trend in a joint's dielectric properties corroborate to the dielectric properties of laminates shown in previous section; this proves that the defect captured by BbDS is interfacial.

4.2.1 Evolution of volume defect and corresponding BbDS values

Changes in real permittivity due to volume defects samples with release film inserts are plotted below:

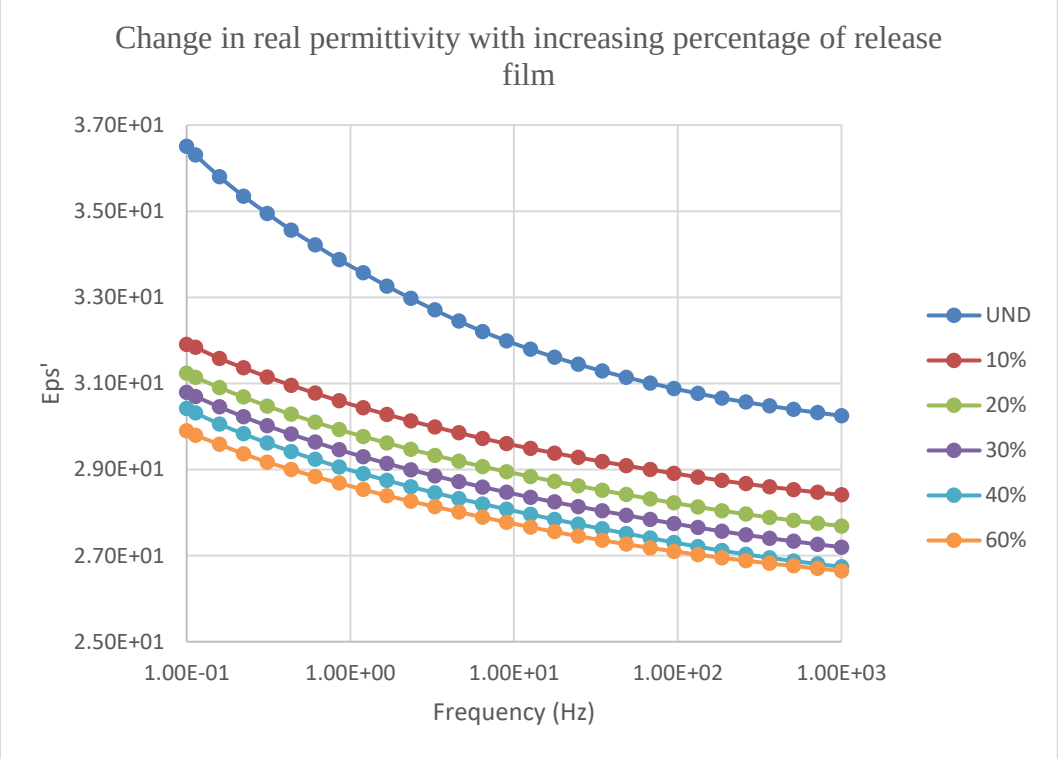

Figure 4.7 Change in real permittivity with increasing percentage of release film in overlap joint

The trend of real permittivity in volume defects is completely opposite from that of surface defects, which not only determine that BbDS can determine damaged and undamaged joints specimen, it can also capture type of damage present in the specimens.

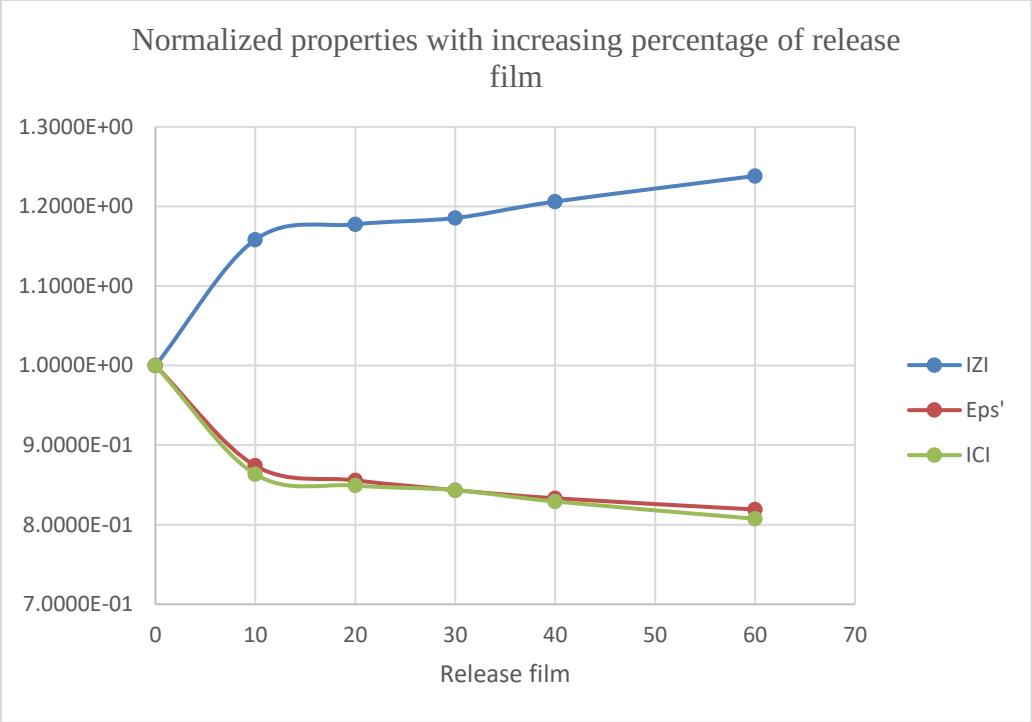

Figure 4.8 Change in normalized properties with increasing percentage of release film in overlap joint

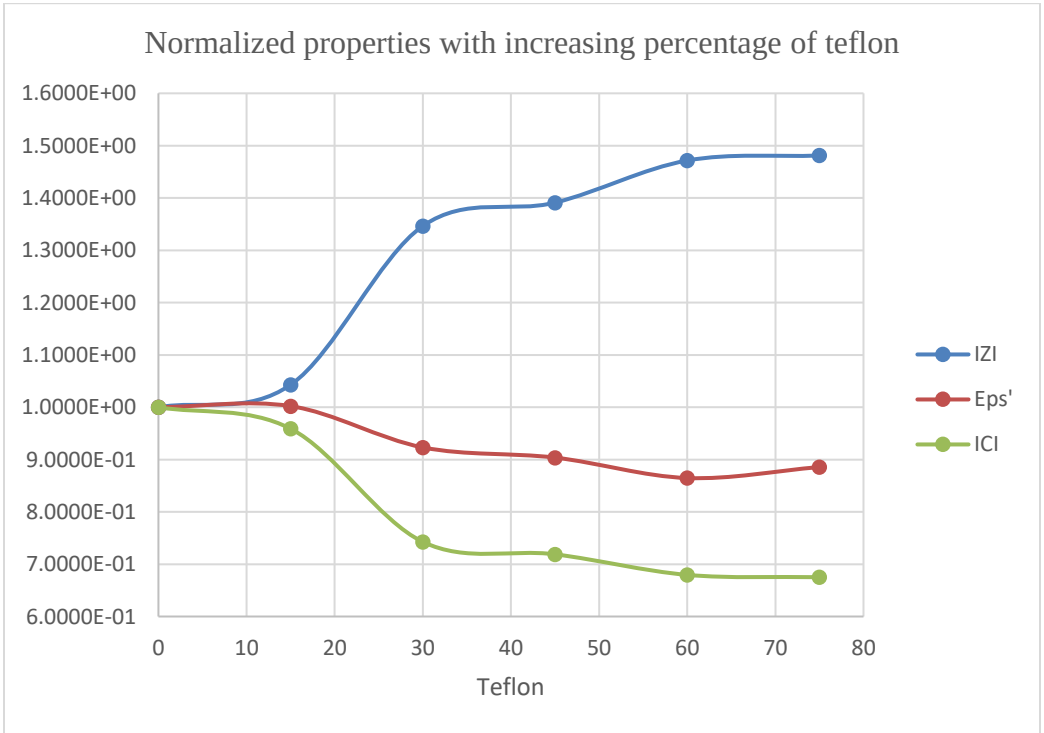

Figure 4.9 Change in normalized properties with increasing percentage of release film in overlap joint

Dielectric properties were normalized and plotted against the percentage of teflon and release film in specimens as seen in figure 4.8 and 4.9.

4.3 Summary and observation

The testing carried out in this study has demonstrated the usefulness of broadband dielectric spectroscopy, as well as accessing the type interfacial defects. The trend suggests significant changes in dielectric properties due to the type of surface modifications. Impedance values shown good correlation with the type of defects, especially in frequency range below 1 Hz.

CHAPTER 5

MECHANICAL DURABILITY OF JOINTS WITH WEAK INTERFACE

In the previous chapter, we studied the effect of interfacial defects on dielectric properties of overlap joints. The result shows that BbDS technique was able to capture those defects. We will continue our study of adhesive bonds with single lap joints prepared with weak interface. It is a challenge to create a weak bond whose strength can be characterized by a measurable parameter. Numerous techniques have been employed by the researchers as cited in literature to create weak bonds. In this study we manufactured controlled weak joints specimen with zero volume defects and studied their mechanical and dielectric behavior.

5.1 Remaining tensile strength of weak joints

Single lap adhesively bonded joints were prepared with “weak” adhesive bond and tested for residual tensile strength and then compared to undamaged single lap joints. Five specimens of each kind were made for this study.

5.1.1 Specimen preparation

Single lap adhesively bonded joints were manufactured according to ASTM D5868 [1]. Two different groups of specimens were made by modifying one bond surface of one group of samples. Weak joints were made by applying Fibrelease agent (FRA) three times on bond surface of one laminate. The release agent was only applied to the bonding area of laminate. 1/8” Quasi isotropic carbon fiber laminate was used to make

the specimens shown in figure 5.1. The procedure to make adhesive bonds was discussed in chapter4.

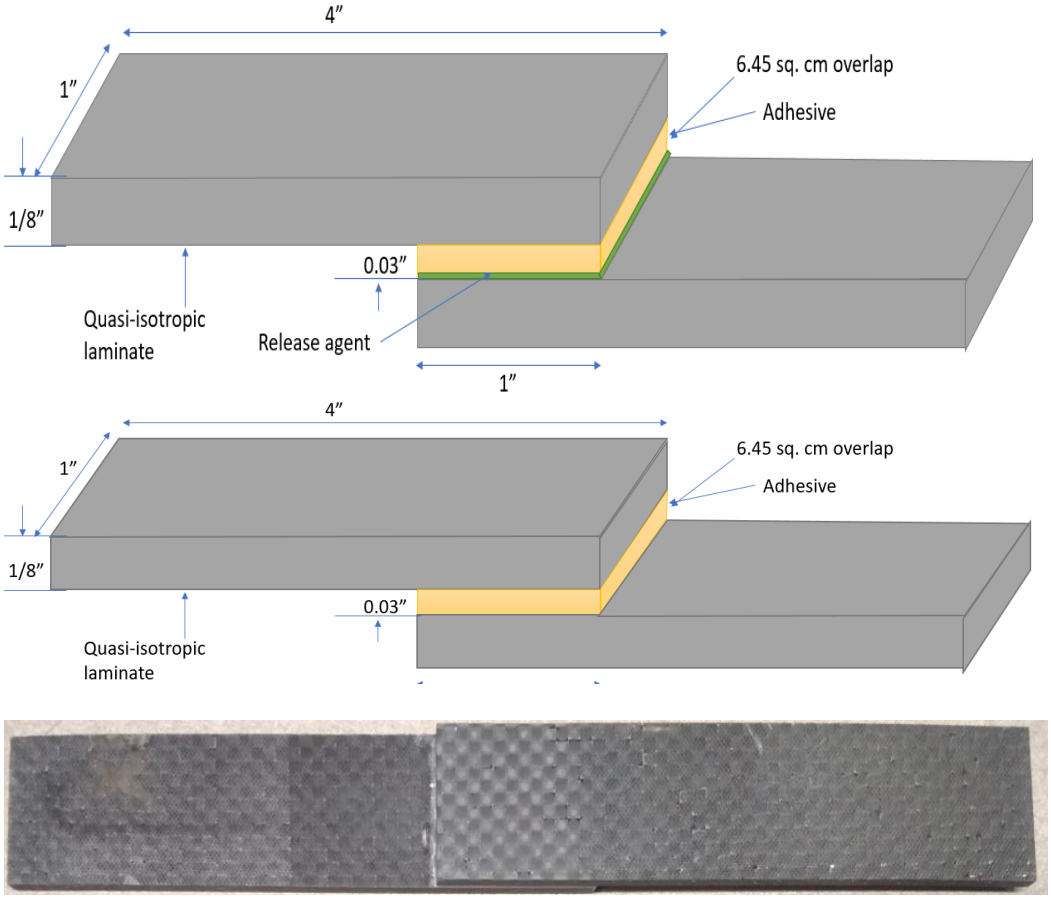

Figure 5.1. "weak" (top) and undamaged (middle) and image of single lap joint (bottom) as per ASTM standards

5.1.2 Remaining mechanical properties

All the specimens were subjected to tensile test to determine the variation in their mechanical properties caused by "weak" bonds. Because it is very difficult to detect the weak bond, the specimens were loaded to failure in MTS machine. All tests were done following protocol and specifications mentioned in ASTM D5868-2014, which involves tensile testing of single lap joints consist of adhesive bonding two adherent substrates with overlap area over $1"^2$. The sample loading was explained in figure 5.2, tabs made of

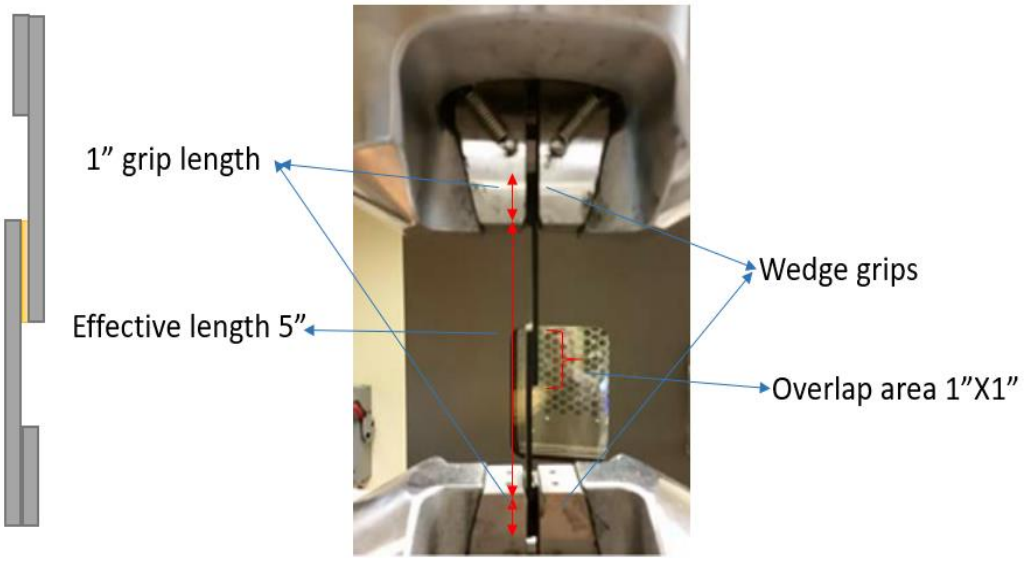

Figure 5.2. Cross section of Single lap joint (left) and experimental setup for tensile testing

1/8” quasi isotropic CFRP (same as adherent in joint) attached each to both ends for proper gripping alignment. The grip length was 1” on both side and effective length of sample was 5”. All five samples from each weak and undamaged group were tested at loading rate of 100 N/sec till failure.

5.1.3 Results and discussion

A lot of research has bseen done on failure modes of adhesively bonded joints, focusing heavily on failure parameters. A lot of predictive failure models developed [2-5] to capture the different failure modes of adhesively bonded joints, which was also discussed in chapter 1.

The load-displacement curve for each group of specimens was obtained from the tensile test and post-processed to determine the shear strength of the bonded joints. The peak load of each sample was determined from the curve in figure 5.4. To compare both the cases better, the axis values of graph are maintained similar. It can be inferred that weak bond joint formed poorly compared to undamaged one. The average shear strength values

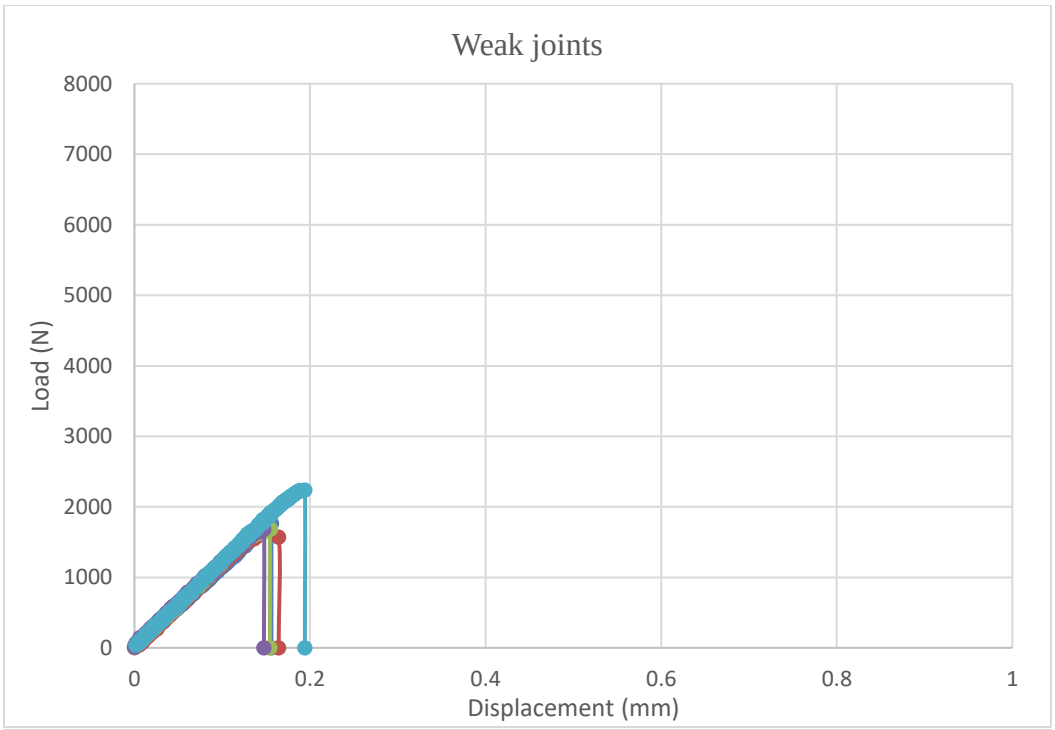

Figure 5.3. Load vs displacement response of weak joint (top) and undamaged joint (bottom)

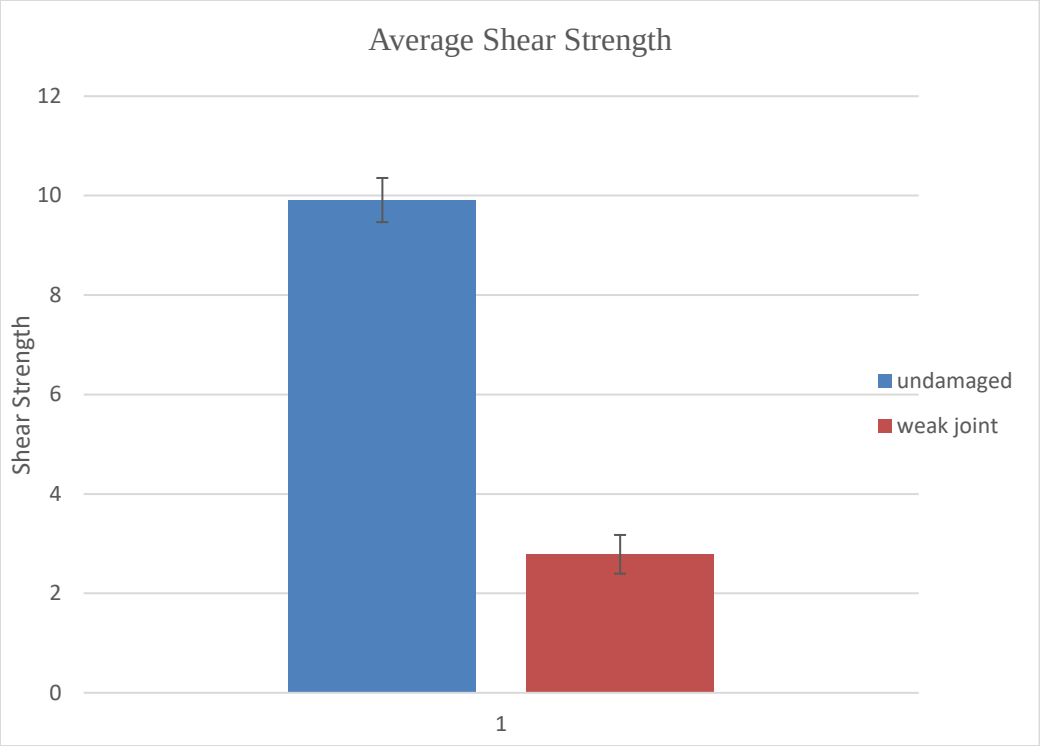

Figure 5.4. Average shear strength of weak and undamaged specimens

of the joints were calculated from the load-displacement curve for both the type of bond and presented in figure 5.4.

Figure 5.5 shows the image of specimen (taken from phone camera) after failure on MTS. It shows that the failure mode of weak joint was adhesive failure whereas in the case of an undamaged joint, there was cohesive failure in all the joints tested. The fibrelease coating, applied to prepare weak bond, is also visible in the figure, which indicates interfacial failure. Undamaged specimens show good bond quality.

5.2 Mechanical strength and dielectric properties

The objective of this chapter is to use broadband dielectric spectroscopy to nondestructively measure the characteristics of weak bonds and compare it with the undamaged ones. Earlier work by Clifford. J. et al. [6], worked on capturing the changes in mechanical properties with low velocity impact damage by dielectric properties. In this

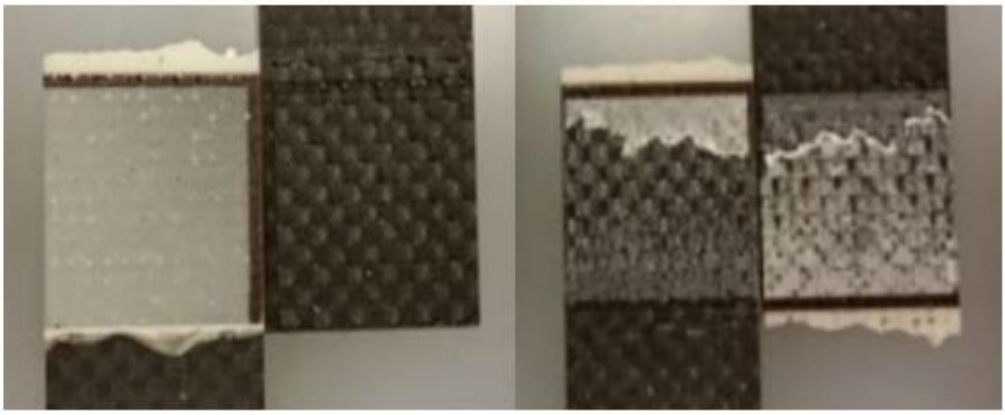

Figure 5.5 Specimens after failure in MTS with weak joints (left) and undamaged joints (right)

work, we will co-relate the remaining residual strength with changes in dielectric properties of the lap joints with weak joint.

5.2.1 Specimen and testing measurement

In this experiment, the similar lap joints are used as in previous section. Novocontrol is used to measure the dielectric properties of both weak and undamaged specimens, as described in chapter 3. Then The 1”X1” copper electrode used to do the measurement will cover the joint area of specimens as shown in figure 5.6. Mechanical testing carried out earlier will be used to relate the degradation of strength with surface modification with dielectric behavior.

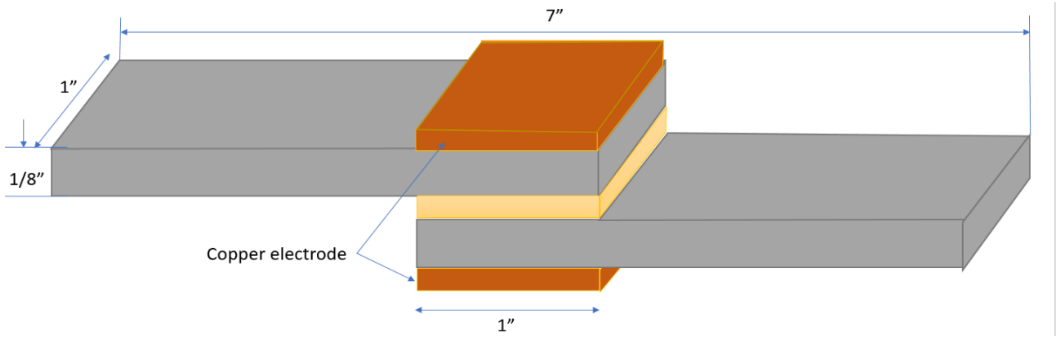

Figure 5.6. specimen-electrode assembly for BbDS

5.2.2 Visualization methods

Images of specimen were taken in MicroXTC-400 3D-Xray microscope (figure 5.7) to understand the bonding between adherent and adhesive. The images were taken in 20X magnification to allow us to see the interface of joints.

Figure 5.7. MicroXTC-400

5.2.3 Results and discussion

As discussed, weak joints were made by modifying one surface of bonding surface of adherent. For these specimens, bulk BbDS measurements are taken and changes in complex permittivity with frequency for both kind of specimens looked at (figure 5.8). It is clear from the figure 5.3 that there is significant difference in both real and imaginary permittivity between weak and undamaged joint. We can safely assume that BbDS is able to capture the interfacial defect present in the weak bond. From the graph above, it is apparent that the changes in values due to weak adhesive bond are higher at low frequency, such as at 0.1 Hz. Five specimens of each bond type were tested and the result were very consistent.

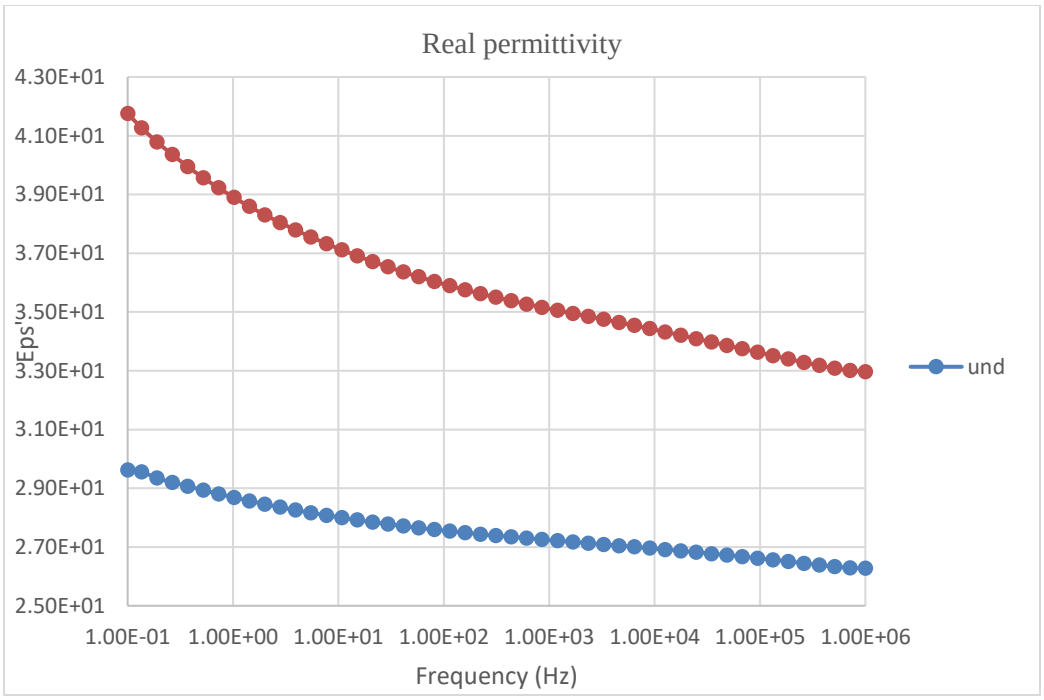

Figure 5.8. Real and imaginary part of frequency as a frequency function

Figure 5.9 shows the change in impedance at 0.1 Hz frequency of specimens due to weak adhesive bond.

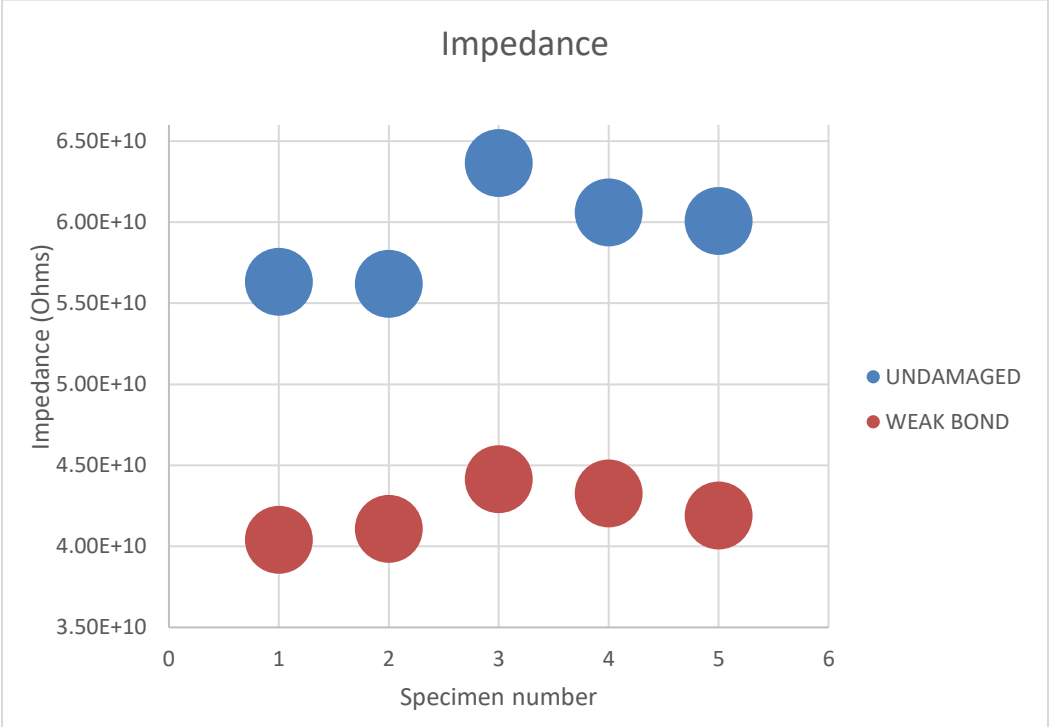

Figure 5.9 Change in AC impedance at 0.1 Hz of lap joint due to interfacial defect

Now, we compare the changes we captured in dielectric properties with shear strength of damaged samples we measured in previous section. All five weak joint specimen's properties are compared. Dielectric properties at set frequency of 0.1Hz with shear strength are normalized and plotted in figure 5.10 below.

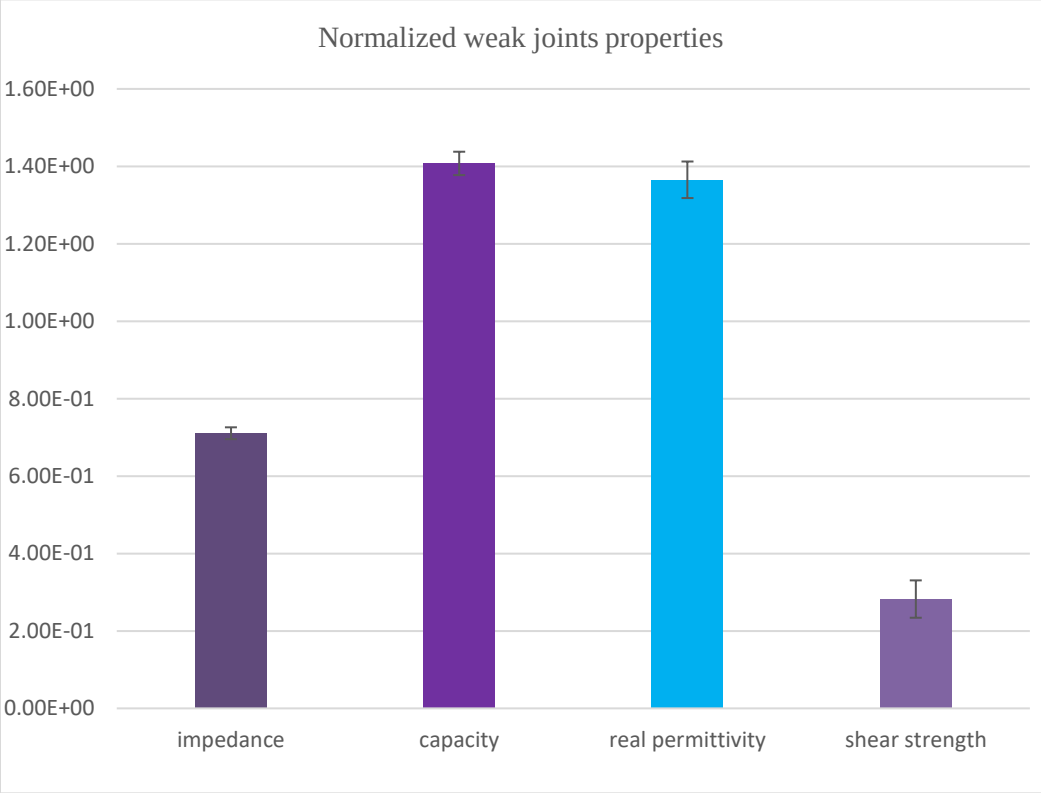

Figure 5.10. Change in normalized properties in weak joints specimens

From the graph above, we can conclude that the changes in properties are very consistent and can be used to determine the interfacial defect. Also, the graph demonstrates that capacity and real permittivity are more sensitive to interfacial damage compared to other dielectric properties.

3D images of joint specimen were taken to examine the adhesive bond formation using 3D X-ray microscopy.

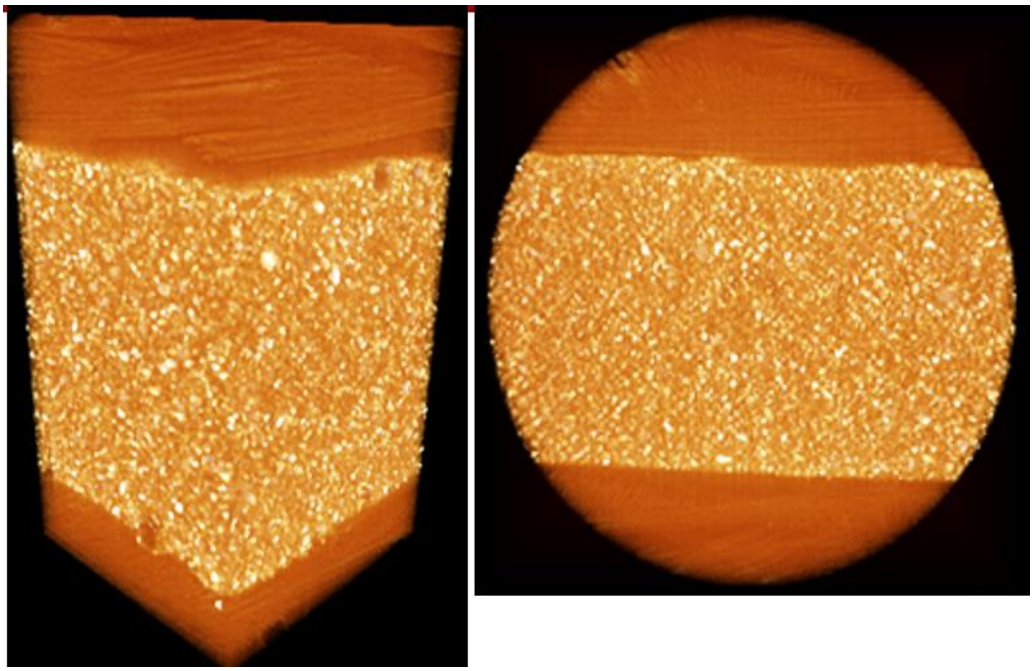

Figure 5.11. X-ray images of single lap joint specimen.

5.3 Summary and observation

In this chapter, controlled weak lap joints were made by making modification on one bond surface and measured for changes in its mechanical and dielectric properties. Strength tests were conducted to measure the remaining mechanical properties of weak lap joints. Non-destructive Broadband dielectric spectroscopy was used to measure the frequency dependent response of single lap joint specimens with interface defect. Dielectric properties were shown to capture the interfacial defects of adhesive bonds and a relationship has been formulated between dielectric and remaining mechanical properties.

REFERENCE

1. ASTM(D5868-014). Standard test method for lap shear adhesion for fiber reinforced plastic (frp) bonding. 2014
2. Kim KS, Yoo JS, Yi YM, Kim CG. Failure mode and strength of uni-directional composite single lap bonded joints with different bonding methods. Compos Struct 2006;72(4):477–85.
3. Kairouz KC, Matthews FL. Strength and failure modes of bonded single lap joints between cross-ply adherends. Composites 1993;24(6):475–84.
4. Cheuk PT, Tong L. Failure of adhesive bonded composite lap shear joints with embedded precrack. Compos Sci Technol 2002;62(7–8):1079–95.
5. Kumar SB, Sivashanker S, Bag A, Sridhar I. Failure of aerospace composite scarfjoints subj
6. Clifford, J., (2015) “dielectric characteristics of microstructural changes and property evolution in engineered materials”, Thesis, University of South Carolina
7. Belingardi, G., Brunella, V., Martorana, B., Ciardiello, R., “Thermoplastic Adhesive for Automotive Applications”, Adhesives - Applications and Properties, Chapter 13, 2016

CHAPTER 6

ANALYTICAL FORMULATION OF DIELECTRIC AND MECHANICAL PROPERTIES OF BONDED JOINTS

Adhesively bonded joints considered in this study used carbon fiber reinforced epoxy composite laminate as adherend and two-part room temperature cured epoxy paste adhesive system in a single lap joint configuration. As outlined in earlier chapter, ASTM 5868 standard was followed which created a short overlap (25.3 mm inch by 25.4 mm) with thin adherends (3 mm) and moderately thick adhesive (0.75 mm). This test method is useful for generating comparative apparent shear strength data for joints made from a number of FRP materials, providing a means by which FRP surface treatments may be compared. Experimental results have shown that weak interface significantly reduces failure load and also changes failure mode from cohesive/interphase to interface failure. This shift in failure mode is the hallmark of loss of ductility and formation of a brittle joint. In this chapter, the objective is to identify simplest approximate analysis tools that can reliably characterize mechanical behavior single lap joint (with or with weak interface) and perhaps use it for parametric studies (properties of adhesive and adherends, joint dimensions.

On the other hand, the adhesive joint consists of a dielectric adhesive sandwiched between two moderately conductive composite adherends. The observed bulk response was similar to a capacitive behavior as expected. The surface modification of the adherends changed the dielectric characteristics of the joint and results were discussed in

earlier chapters. The reason for different dielectric response of joint with weak interface was due to change in interfacial polarization as one of the adherend-adhesive (conductor-insulator) material boundary. An approximate formulation is desired to capture the dielectric property variation of single lap joint in the AC frequency domain (0.1 Hz to 1 MHz). This is another key objective of this chapter and discussed in a later section.

6.1. Simple Analytical Models of Lap Joints

Different analytical methods of varying complexities are available in the literature for the calculation of stress distributions in adhesively bonded joints and few excellent review papers [1-6] have summarized those formulation with extensive details. In addition, there are numerous numerical studies using finite element method have been reported in the literature but those are not of direct interest here. There are three important controlling factors which may help decide what level of complexity may be required: 1) failure mode (cohesive in adherend, adhesion at interface/interphase, cohesive in adhesive) 2) Potential for adherend bending and transverse shear 3) anisotropic adherend and nonlinearity in adhesive response. The third factor obviously will require numerical solution and usually improves accuracy. For cohesive or interphase failure within the adhesive, some adherend bending and transverse shear is expected. However, this bending effect is minimal for short overlap length and increases with the length of the joint. The failure may be due to a combination of peel and shear stresses. Excellent quantitative description of relevant joint configuration parameters is available in ref [4]. On the other hand, if the failure mode is interfacial, then the joint acts in a brittle manner and there is not significant bending of adherend. The failure is often shear dominated. Considering the above understanding, two simplistic closed-form analytical methods will be examined here: one based one shear lag

concept and the based-on beam on elastic foundation concept to account for shear-peel coupling due to adherend bending.

6.1.1. Volkersen Shear Lag Model

The most common shear lag based analytical in literature was developed by Volkersen and this linear elastic model only considers shear stress. The bending effect caused by the eccentric load path in a lap joint is not considered. The basic joint configuration is shown in figure 1 below.

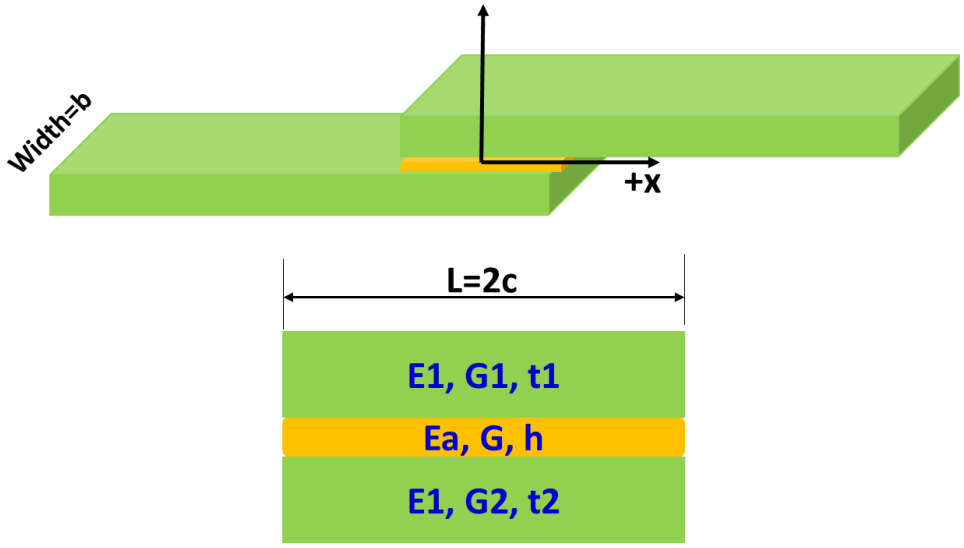

Figure 6.1 Single lap joint configuration for Volkersen shear lag model

The shear stress distribution is given by the following expression which predicts maximum shear stress at the end of the overlap.

$$\tau volkerson(P, x) := \frac{\frac{P}{b}\cdot\omega}{2\cdot\sinh\left(\frac{\omega\cdot L}{2}\right)}\cdot\cosh(\omega\cdot x)+\frac{\frac{P}{b}\cdot\omega}{2\cdot\sinh\left(\frac{\omega\cdot L}{2}\right)}\cdot\left(\frac{E2\cdot t2-E1\cdot t1}{E1\cdot t1+E2\cdot t2}\right)\cdot\sinh(\omega\cdot x)$$

Here, P is the applied tensile load and ω is the characteristic shear lag parameter given by the following:

$$\omega := \sqrt{\frac{G}{h} \cdot \frac{E2 \cdot t2 + E1 \cdot t1}{E1 \cdot t1 \cdot E2 \cdot t2}}$$

Although the joint ends should be stress free, the maximum values at the end should be interpreted as stress at a point just near the edge. Some researchers have treated it as average stress criteria by averaging over a distance equal to the adhesive thickness. TOM modification to Volkersen involves a different shear lag parameter to include adherend shear effect and implemented using a parameter (α) which depends on shear modulus of adherend/adhesive. For α=1, there is no adherend transverse shear effect on the shear stress distribution.

$$\beta := \frac{\omega}{\sqrt{1 + \frac{G}{h} \cdot \left(\frac{t1}{3 \cdot G1} + \frac{t2}{3 \cdot G2}\right)}} \qquad \alpha := \frac{1}{\sqrt{1 + \frac{G}{h} \cdot \left(\frac{t1}{3 \cdot G1} + \frac{t2}{3 \cdot G2}\right)}}$$

For the ASTM 5868 configuration and properties of chosen material system (carbon fiber reinforced epoxy laminate and epoxy adhesive), the adherend shear effect was found to be quite negligible in Volkersen formulation.

6.1.2. Goland and Reissner (GR) Model

Goland and reissner model consider adherend bending effect due misaligned load path of a single lap joint configuration as shown in figure 2.

For a lap joint with overlap length, 2c (L=2c) and adherend thickness t (t1=t2=t) subjected to applied load, p per unit width (p=P/b), the shear stress distribution are given by the following equations:

$$\tau GR(P, x) := \frac{p \cdot 1}{8 \cdot c} \cdot \left(\frac{\beta \cdot c}{t} \cdot (1 + 3 \cdot k(P)) \cdot \frac{\cosh\left(\frac{x}{c} \cdot \frac{\beta \cdot c}{t}\right)}{\sinh\left(\frac{\beta \cdot c}{t}\right)} + 3 \cdot (1 - k(P)) \right)$$

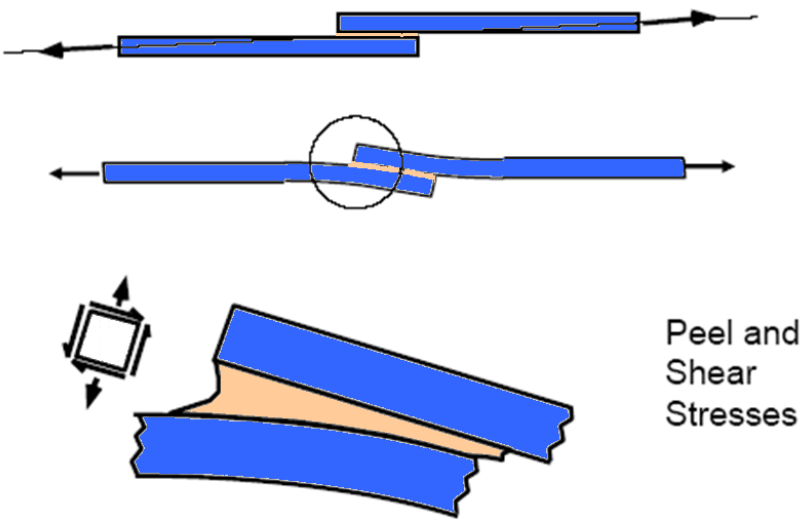

Figure 6.2 Single lap joint configuration for Goland and Reissner Shear-Peel Coupling model

Here, k is the edge bending moment factor. TOM modification [4] again changes β to include adherend shear deformation effect defined by a parameter (α). For the present joint configuration, there is some adherend shear deformation effect and may be considered. In TOM modification, k is very close to 1 and often taken as 1.

$$\alpha GR := \frac{1}{\sqrt{1 + \frac{2 \cdot G \cdot t}{3 \cdot h \cdot G1}}}$$

$$\alpha GR := \frac{1}{\sqrt{1 + \frac{2 \cdot G \cdot t}{3 \cdot h \cdot G1}}}$$

$$\beta GR := \alpha GR \cdot \lambda GR$$

$$\tau GRTOM(P, x) := \frac{p \cdot 1}{8 \cdot c} \cdot \left(\frac{\beta GR \cdot c}{t} \cdot (1 + 3 \cdot k) \cdot \frac{\cosh\left(\frac{x}{c} \cdot \frac{\beta GR \cdot c}{t} \right)}{\sinh\left(\frac{\beta GR \cdot c}{t} \right)} + 3 \cdot (1 - k) \right)$$

A plot of shear stress distribution with Volkersen, GR and GR-with TOM modification is shown in figure 3. The lap shear strength data (24MPa) form manufacturer has been used as failure criteria. There are significant ambiguity regarding proper failure

criteria. Without lack of custom experimental data on adhesive, it is not possible to apply a different criterion at this time. However, the present approximation provides very reasonable estimate. Experimental failure load was about 6049 N and the predictions look very close from GR-Tom model.

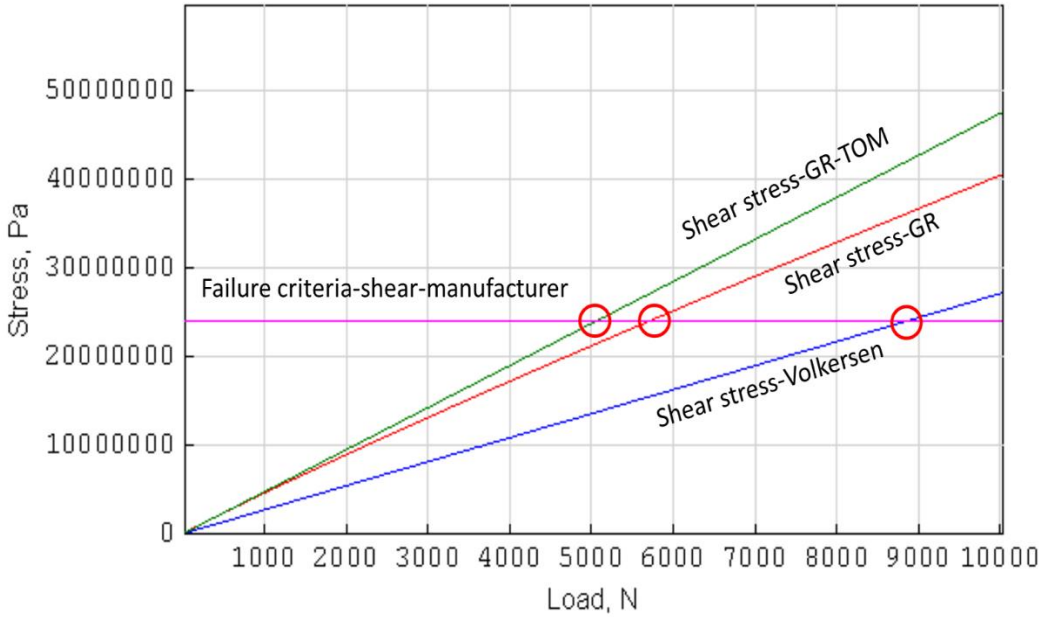

Figure 6.3 maximum shear stress as a function of applied load for base joint

For weak interface, it is reasonable to assume that the adherend and adhesive do not yield at all. Specifically, the adhesive act like a brittle manner and do not undergo significant shear deformation due to lack of support from the weak adherend interface. We postulate that once it tries to shear beyond linear strain limit, the weak interface fails before allowing adhesive to shear. Hence, we take the linear strain limit of adhesive (about 0.0022) as the failure criteria instead of shear strength in a strongly bonded joint. With 3.19GPa adhesive modulus, this gives about 7MPa as the limiting stress level or failure criteria.

This choice of failure criteria is reasonable from another point of view. In chapter-3, work of adhesion was calculated for modified and base laminate surface. The work of

adhesion for weak surface is about 3 times lower than that of base laminate. So reduction of lap shear strength (failure criteria) by about a factor of 3 will yield 8 MPa which is close to 7 MPa chosen as the failure criteria with approximate linear strain limit. The results are plot in the following figures and intersections of failure criteria with max stresses are the failure loads.

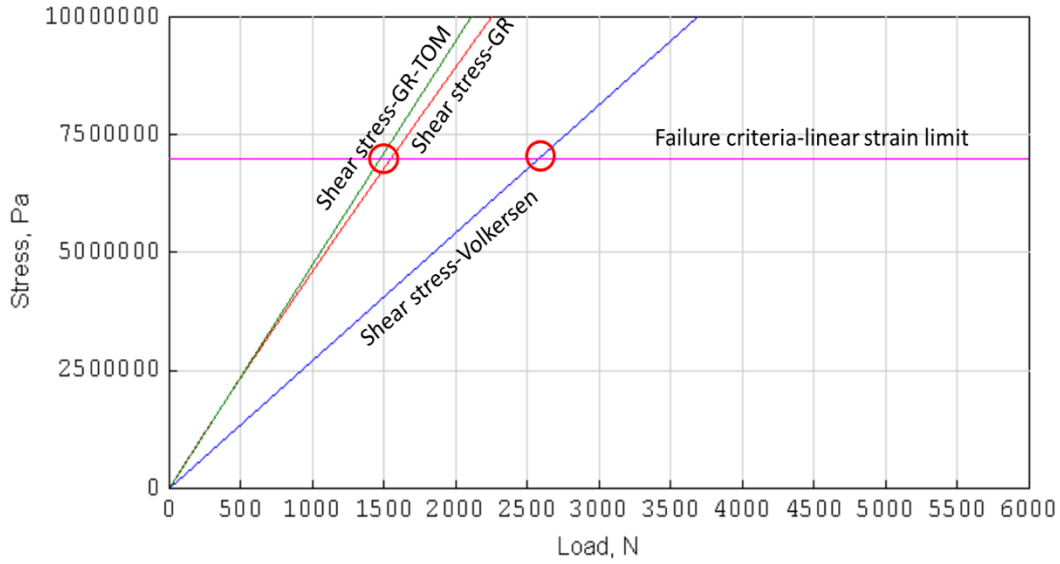

Figure 6.4 maximum shear stress as a function of applied load for weak interface

Table 6.1 Summary of Failure Load

	Failure load, N			
Joint Type	Volkersen	GR	GR-TOM	Experiment ave
Base lap joint	8850	5700	5100	6049
lap joint-weak interface	2575	1550	1475	2200

6.2. Dielectric Property Prediction Model for Bonded Joints

Dielectric properties of laminated joints depend on frequency dependent properties of adherend and adhesive. It is understood that the joint will act as capacitor and hence

contribution from adhesive will dominate the low frequency response. Considering electrode polarization constant in base joint and modified joint, the major polarization will occur at material boundaries. Specifically, the adherend-adhesive interface polarization will differentiate the base joint and the weak interface joint. The weak interface will have a different polarization characteristic due to two major reasons: 1) chemical bonding is different ii) roughness and wettability are different.

6.2.1 Impedance Model of Equivalent Joint

Considering above mechanisms, the objective here to develop a simplistic model for predicting response of lap joint using adherend and adhesive properties. We will present Impedance magnitude model first and future development will include complex variable quantities (real and imaginary part isolation). The model does not include stray capacity and line effects. Hence marginal difference in values are expected but the focus is on capturing the trend.

The proposed model for equivalent impedance magnitude of the lap joint can be written as:

$$Zeq(f) := \frac{\omega(f)}{Zahigh} + \frac{Zalow}{\omega(f)} + \frac{1}{Z1} + \frac{1}{Z2}$$

Here, ω(f)= angular frequency, Zalow= impedance of adhesive at lower limit of frequency (fmin), Zahigh= impedance of adhesive at higher limit of frequency (fmax), Z1 and Z2 are frequency-independent impedance of conductive carbon fiber/epoxy laminate. It is to be noted that the Zalow and Zahigh data points will depend on adhesive thickness (or volume fraction of adhesive).

For the weak joint, only one of the adherend-adhesive interface is modified. We postulate that the polarization at this weak interface will change but will follow a similar form of the low frequency contribution of adhesive to equivalent joint impedance. In addition, the separation distance or thickness of adhesive will also affect this response of modified interface. The weak interface will increase capacity and hence reduce impedance of the system. In lap joint the impedance is mostly reactive although minimal resistive contribution come from laminate only at higher frequency. Hence, we propose an empirical form of equivalent joint impedance as follows and a better estimate of the interface effect could be made in the future with full complex variable formulation.

$$ZeqRA(f) := \frac{\omega(f)}{Zahigh} + \frac{Zalow}{\omega(f)} + \frac{1}{Z1} + \frac{1}{Z2} - \frac{1}{2} \cdot \frac{Zalow \cdot Va}{\omega(f)}$$

Volume fraction of adhesive is defined as thickness ratios of adherend (t1 and t2) and adhesive (ta):

$$Va := \frac{ta}{t1 + t2 + ta}$$

6.2.2 Results of Equivalent Joint model and comparison with experimental data:

The figure below shows how impedance of undamaged base joint and joint with weak interface varies with frequency (semi-log graph in figure 5).

If we look at the low frequency response at 0.1 Hz (figure 6), we can clearly observe the effect of weak interface in the joint.

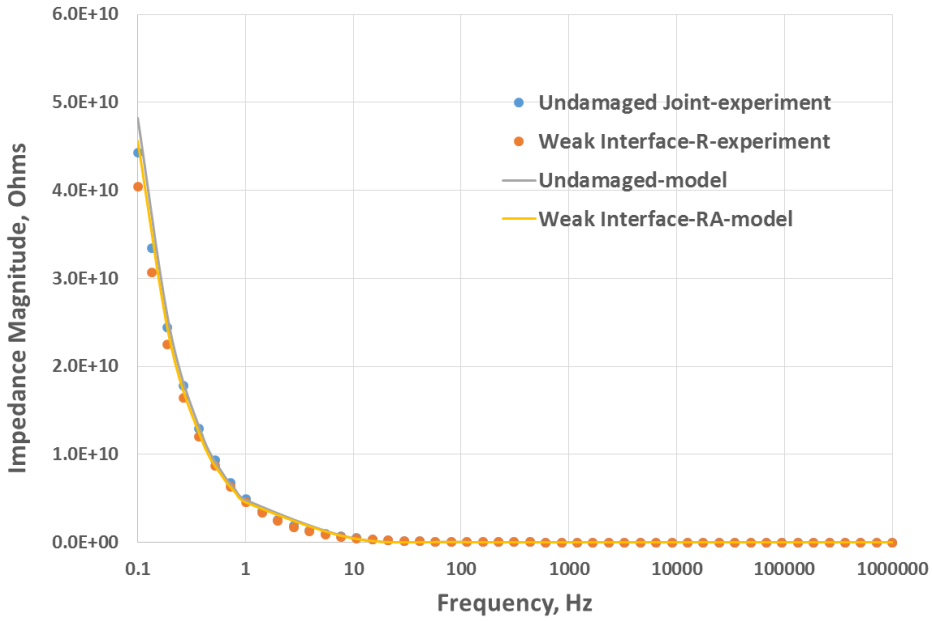

Figure 6.5 Comparison of experiment vs model estimate of impedance magnitude

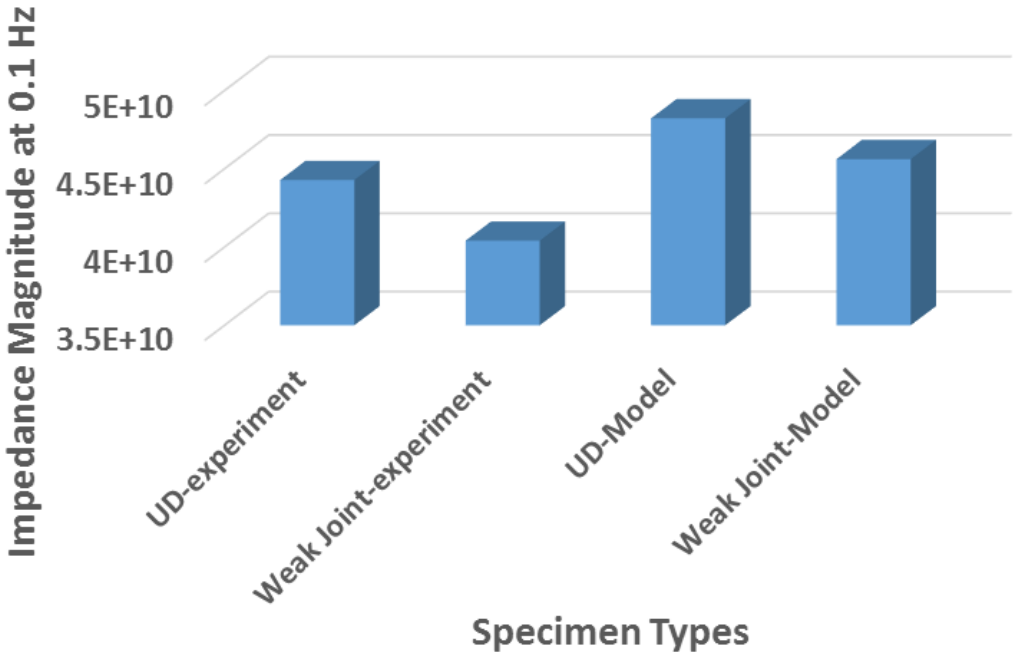

Figure 6.6 Comparison of experiment vs model estimate of impedance magnitude

From the figure 5 and 6, it can be concluded that the empirical approximate model captures the trend correctly. The exact magnitude is expected to be different as the idealized equivalent model do not include circuit losses and exact polarization at adherend-adhesive interface is not known. A future model of permittivity and sample capacity in the complex function domain will be needed to quantify the exact interface effect but the validation remains a change as probe can't be placed at that interface unlike traditional electrode polarization effect (4-probe setup).

6.3 Summary and conclusion

In this chapter, closed form analytical models have been applied to estimate failure load in lap joint with weak interface. The brittle joint model based on shear lag is determined to be best suited to capture the response. The failure criteria used is a simplistic approximation but reasonable one as found to be consistent with work of adhesion studies. More experimental data required to propose a failure criterion for weak interface. The observed estimates of model and experimental data correlates very well.

Dielectric properties of lap joint have been estimated form adhesive and adherend properties using empirical or approximate model. The estimated values differ from experimental data but the trend is consistent. The benefit of such model is that parametric studies can be performed to understand how adhesive thickness and other interface properties may affect dielectric properties of the joint. More sophisticated models may be developed in the future based on this fundamental understanding.

REFERENCES:

1. Budhe, S., et al. 2017. "An updated review of adhesively bonded joints in composite materials," International Journal of Adhesion and Adhesives, 72: 30-42.
2. René Quispe Rodríguez, Paulo Sollero, Éder Lima de Albuquerque, STRESS ANALYSIS AND FAILURE CRITERIA OF ADHESIVE BONDED SINGLE LAP JOINTS. 21st International Congress of Mechanical Engineering October 24-28, 2011, Natal, RN, Brazil.
3. Charles Yang, John S. Tomblin, and Zhidong Guan. Analytical Modeling of ASTM Lap Shear Adhesive Specimens. Report: DOT/FAA/AR-02/130
4. M. Y. Tsai, d. W, oplinger, j.morton. Improved theoretical solutions for adhesive lap joints. lnt. J. Solids Struclures VoL 35, No. 12, pp. 1163-1l85, 1998.
5. Rene´ Quispe Rodrı´guez, William Portilho de Paiva, Paulo Sollero, Marcelo Ricardo Bertoni Rodrigues, der Lima de Albuquerque. Failure criteria for adhesively bonded joints. International Journal of Adhesion & Adhesives 37 (2012) 26–36.
6. Yarrington, P., C. Collier, and B. Bednarcyk, 2006, Failure Analysis of Adhesively Bonded Composite Joints via the Virtual Crack Closure Technique, in 47th AIAA/ASME/ASCE/AHS/ASC Structures, Structural Dynamics, and Materials Conference. American Institute of Aeronautics and Astronautics.

CHAPTER 7

CONCLUSION AND FUTURE WORK

7.1 Summary of results and observations

Adhesive bonding of composite shows promising growth in a wide variety of applications. In this work, we have shown that interfacial defects in composite joints can be characterized by their dielectric properties. Broadband dielectric spectroscopy is shown to be a valuable technique in capturing dielectric property changes. It has shown that the dielectric response is most sensitive at low frequency, i.e. below 1 Hz. We have been able to capture various type of surface modifications on composite laminate surfaces before and after bonding. Unlike previous studies, we have proven that BbDS can be used to capture the effect of defects at the interface of adhesive bond made of carbon fiber adherend.

Contact angle measurements are a proven method to check the wettability of bond surfaces. Carbon fiber laminates under different type of surface modifications were used to do wettability studies to imitate the possibility of impurities on adherend surface before bonding. The change in dielectric properties due to those modification was then captured by BbDS.

Overlap adhesive joints were made with several kinds of surface and volume defects and tested for their dielectric properties. The results show that BbDS was able to capture the change in dielectric properties based on the type of defect. Furthermore, controlled specimens of single lap joint configurations were made with interfacial defect to simulate weak bond with zero volume defect and tested for their bond strength by

loading until failure after testing for their dielectric properties. These dielectric variables associated with weak bonds were assigned to specimens representing the material's state due to interfacial defects. The dielectric measurements are then related to change in bond strength due to defects. The main advantage of this method is that it is completely nondestructive because the applied voltage in BbDS is too low to cause any harm to bond properties.

Analytical models were also used to investigate the estimated failure in lap joints with weak interface and was found to be consistent with work of adhesion. An empirical model was used to estimate that dielectric properties of lap joints are found to be matching the trend of experimental data.

7.2 Potential future extension of work

The work in this thesis is ongoing and further study needs to be done by varying thickness of specimen, measuring effect of different orientation of composite laminates, different types of adhesive joints using broadband dielectric spectroscopy. More sophisticated models needed to be developed by adding more experimental data to predict weak interface.